Impacts of variable versus fixed phytoplankton stoichiometry on the dynamics of biogeochemical models

Dissertation
zur Erlangung des Doktorgrades
der mathematisch–naturwissenschaftlichen Fakultät
der Christian–Albrechts–Universität zu Kiel

vorgelegt von
Lena Göthlich

Kiel 2012

Erster Gutacher: Prof. Dr. Andreas Oschlies
Zweiter Gutachter: Prof. Dr. Ulrich Sommer

Tag der mündlichen Prüfung: 4.12.2012
Zum Druck genehmigt: 4.12.2012

gez. Prof. Dr. Wolfgang J. Duschl, Dekan

To Stephan

Contents

List of Figures

List of Tables

Summary

For marine biogeochemical models used in simulations of climate change scenarios, the ability to account for adaptability of marine ecosystems to environmental change is crucial. Biogeochemical models commonly include a single all–encompassing phytoplankton that represents the average community and does not exhibit any physiological flexibility, e.g. in stoichiometry. While these models succeed at reproducing e.g. global chlorophyll distribution, dynamics emerging from adaptation are lacking. Those dynamics feed back into the climate system via the biological pump and are key to assessing the ocean's response to climate change. Therefore, more adaptive pelagic ecosystem models are built via two methods: (1) increasing physiological detail, or (2) resolving communities. Both approaches are investigated in this thesis, particularly with respect to the representation of phytoplankton elemental composition and its effect on model performance.

In part one, an adaptive single–phytoplankton model in a fixed N:C version and an optimality–based flexible N:C version are used to simulate the annual cycle at a subtropical gyre site. Both model versions can be fitted to the annual cycle data, but only the optimality–based model reproduces independent observations. The fixed N:C version fails to capture essential characteristics of the independent datasets since it lacks the flexibility to capture the local nutrient-limited dynamics.

In part two, a community–resolving model that originally employs a common fixed stoichiometry for all species is subjected to interspecific stoichiometric variation. According to resource competition theory, the maximum number of coexisting species at equilibrium equals the number of limiting resources. Yet, like in many community–resolving models, diversity in the original model is often lower, which is critical since diversity is needed to assess changes in community compositions. In agreement with resource competition theory, which states that identical stoichiometry for all species impedes coexistence, it is shown that interspecific stoichiometric variation can significantly increase diversity. Resource–competition theory assumes equilibrium, but in part three of the thesis the previously gained results are shown to be valid also for disturbed systems.

Assessing future ocean biogeochemical responses requires the full adaptive potential of pelagic ecosystem models. In this thesis, fixed phytoplankton stoichiometry is shown to impede the adaptive potential of per se adaptive pelagic ecosystem models. Consequently, allowing for stoichiometric variation provides a straightforward means of significantly improving model capabilities.

Zusammenfassung

Marine biogeochemische Modelle, die in Simulationen von Klimawandel–Szenarien eingesetzt werden, müssen die Anpassungsfähigkeit mariner Ökosysteme wiedergeben. Phytoplankton wird in gewöhnlichen Biogeochemischen Modellen als eine einzige allumfassende Art dargestellt, die die durchschnittliche Phytoplankton–Gemeinschaft repräsentiert. Deren physiologische Eigenschaften sind konstant, so ist z.B. die Stöchiometrie unveränderlich. Derartige Modelle reproduzieren zwar z.B. die globale Chlorophyll–Verteilung, können jedoch biologische Adaptation und daraus entstehende Veränderungen nicht wiedergeben. Über die biologische Pumpe existiert eine Rückkopplung der biologischen Prozesse an das Klima, deshalb ist ihre Repräsentation in Modellen unerlässlich, wenn die Reaktion der Ozeane auf den Klimawandel eingeschätzt werden soll. Daher werden auf zwei Wegen adaptive Modelle pelagischer Ökosysteme konstruiert: (1) durch die Darstellung physiologischer Prozesse und (2) durch die explizite Darstellung von Diversität. In der vorliegenden Arbeit werden beide Ansätze untersucht, mit besonderem Schwerpunkt auf der Darstellung von Phytoplankton–Stöchiometrie und deren Einfluss auf das Modellverhalten.

In Teil eins werden zwei Versionen eines adaptiven Phytoplankton–Modells, davon eine mit konstanter und eine mit variabler Stöchiometrie, benutzt um einen Jahresgang im subtropischen Ozean zu simulieren. Beide Modellversionen können an die Jahresgang–Daten angepasst werden, hingegen reproduziert nur die Version mit variabler Stöchiometrie auch unabhängige Daten. Entscheidende Merkmale des unabhängigen Datensatzes kann die Version mit festgelegter Stöchiometrie nicht reproduzieren, da hier die nötige Flexibilität fehlt um die Auswirkungen der lokalen Nährstofflimitierung abzubilden.

In Teil zwei wird in einem globalen Modell, das explizit Phytoplankton–Diversität auflöst und ursprünglich eine identische Stöchiometrie für alle repräsentierten Arten festlegt, die Stöchiometrie zwischen den verschiedenen Arten variiert. Nach der Theorie der Ressourcenkonkurrenz können im Gleichgewicht so viele Arten koexistieren wie es limitierende Ressourcen gibt. In dem verwendeten Modell ist jedoch, wie auch in anderen Modellen mit expliziter Phytoplankton–Diversität, die Anzahl der koexistierenden Arten oft deutlich kleiner als die Anzahl der limitierenden Ressourcen. Der Erhalt von Diversität im Modell ist jedoch unerlässlich, wenn es darum geht durch den Klimawandel verursachte Änderungen in der Artenzusammensetzung abzuschätzen. Gemäß

der Theorie der Ressourcenkonkurrenz, die besagt, dass identische Stöchiometrie den Erhalt von Diversität verhindert, wird in Teil zwei gezeigt, dass Unterschiede in der Stöchiometrie verschiedener Arten die Diversität deutlich erhöhen. Obwohl die Theorie der Ressourcenkonkurrenz von einem Gleichgewichtszustand ausgeht, wird darauf folgend in Teil drei gezeigt, dass die in Teil zwei erzielten Ergebnisse auch auf Systeme übertragbar sind, die Störungen ausgesetzt sind.
Um zukünftige Reaktionen des Ozeans abzuschätzen, wird das maximale adaptive Potenzial von biogeochemischen Modellen benötigt. Die vorliegende Dissertation zeigt, dass festgelegte Stöchiometrie das adaptive Potenzial von an sich adaptiven Modellen einschränkt. Daraus folgt, dass das explizite Auflösen von variabler Stöchiometrie eine vergleichsweise einfache Methode darstellt die Leistungsfähigkeit biogeochemischer Modelle deutlich zu steigern.

1 Introduction

1.1 Motivation

The ocean plays a key role in the earth's climate system, particularly with regard to the global carbon cycle. A large amount of carbon is stored in the ocean as inorganic carbonates and CO_2, primarily in the deep ocean (Falkowski et al., 2000), which has no direct exchange interface with the atmosphere. Atmospheric CO_2 enters the deep ocean via two distinct mechanisms: the physical pump and the biological pump (Raven and Falkowski, 1999). The physical pump, also called the solubility pump, comprises the direct sinking of CO_2–rich water from the surface to the deep ocean in regions of deep water formation, e.g. in the North Atlantic: warm surface water, which is in direct exchange with the atmosphere, reaches the subpolar North Atlantic with the Gulf Stream and cools down. Since solubility of CO_2 is inversely related to temperature, its concentration in the surface water then increases through the dissolution of more atmospheric CO_2. This water, now rich in CO_2, sinks due to the cooling, taking atmospheric CO_2 with it and thus removing it from the atmosphere.

The biological pump is based on phytoplankton photosynthesis in the ocean surface layer: phytoplankton fixes CO_2 and assimilates it into biomass, which, to some extent, sinks out of the surface layer into the deep ocean, where it is slowly decomposed. Especially in the higher latitudes, phytoplankton CO_2 uptake results in a concentration gradient of CO_2 between the surface ocean and the atmosphere, stimulating oceanic uptake of atmospheric CO_2. Carbon stored in the deep ocean is essentially lost from the atmosphere for several hundred years.

The physical pump helps explain why atmospheric CO_2 levels are considerably lower than to be expected from the amount of burned fossil fuels since the Industrial Revolution (Sabine et al., 2004): the "missing" carbon is continuously removed from the atmosphere and being transferred to the deep ocean. Despite this offset, atmospheric CO_2 levels

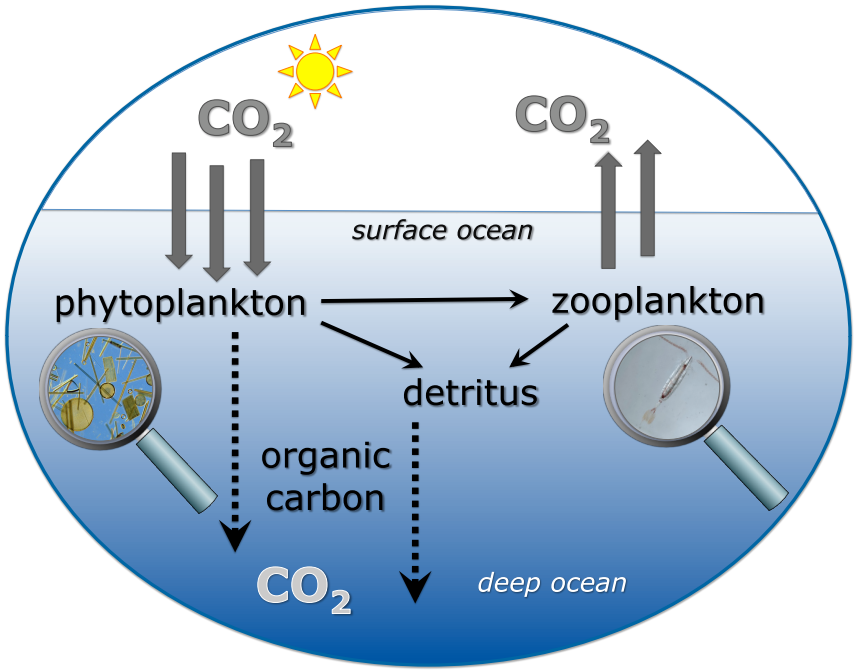

Figure 1.1: Sketch of the biological pump. CO_2 enters the ocean and is converted into biomass via photosynthesis. Part of the biomass is cycled through the food-web and CO_2 is re–released into the atmosphere; part of the biomass sinks into the deep ocean, where it is slowly remineralised to CO_2. Image sources: National Geographic (diatoms), oceanexplorer.noaa.gov (copepod).

have been increasing continuously over the past century due to humans burning massive amounts of fossil fuels. The resulting consequences include global warming, accelerated sea level rise and ocean acidification, which cause drastic changes in the world's social and ecological systems. In particular changes in the pelagic ocean ecosystems in turn feed back into the climate system via the biological pump. The magnitude of the ocean biological response to climate warming is still largely unknown and difficult to quantify, yet it is expected that global ocean primary production will decrease as a result of shallower mixed layers and temperature–driven increases in respiration rates (Riebesell et al., 2009). This involves a decrease in the biological pump, which in turn might escalate the increase in atmospheric CO_2. Additionally, rising upper ocean temperature decreases the solubility of CO_2 , which also decreases the ocean's ability to take up atmospheric CO_2.

Coupled global ocean and climate models are used to assess both the impact of climate warming on physical properties of the ocean, such as water temperature or mixed layer depth, as well as the sensitivity of the biological pump to those changes. Global ocean models typically comprise a biogeochemical model including a pelagic ecosystem model, which come in various levels of complexity (Fasham et al., 1990; Schartau and Oschlies, 2003; Gregg et al., 2003; Follows et al., 2007; Schneider et al., 2008; Pahlow and Oschlies, 2009; Kriest et al., 2010; Sinha et al., 2010; Follows and Dutkiewicz, 2011). However, most descriptions of pelagic ecosystems in coupled ocean and climate models consist of nutrient, phytoplankton, zooplankton, detritus (NPZD) compartments or variants thereof. An example of a simple NPZD model is shown in figure 1.2. While corresponding models succeed at reproducing overall patterns of e.g. global chlorophyll distribution or nutrient levels, they still show weaknesses in certain ocean regions as well as in adequately simulating phytoplankton dynamics emerging from either physiological traits or community dynamics not captured by a single model phytoplankton (Fasham, 1995; Popova et al., 2006).

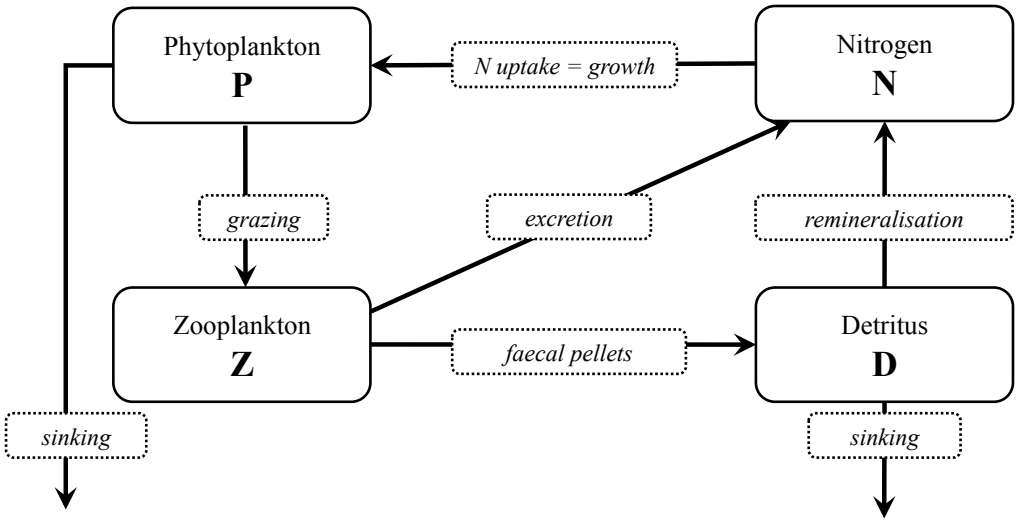

Figure 1.2: Sketch of a simple NPZD model. Boxes indicate bulk variables, arrows indicate elemental fluxes.

Two distinct ways of attempting to increase phytoplankton–related realism in biogeochemical models are: (1) resolving for phytoplankton physiological constraints, which includes explicitly simulating different traits and ratios that are commonly assumed to be fixed, e.g. nutrient uptake parameters, the N:C ratio or the Chl:C ratio (e.g. Pahlow and Oschlies, 2009); (2) explicitly modelling different phytoplankton species or functional types such as diatoms, nitrogen fixers or calcifiers (Sinha et al., 2010). Both approaches essentially aim at simulating a more realistic community response compared to creating a single all–encompassing fixed–trait phytoplankton species that is meant to represent phytoplankton as a whole. The first method simulates a flexible phytoplankton that physiologically adapts to changes in its environment, yet on timescales that essentially represent species succession rather than intraspecific adaptation. The second approach fixes traits within the species, but allows for competition between different phytoplankton types, thereby allowing adaptation on a community scale.

A major issue concerning the explicit resolution of phytoplankton diversity in models is the maintenance of that diversity: Frequently, one species outcompetes one or all of the others, at least regionally, and thus the adaptive potential of the remaining phytoplankton is essentially lost (Gregg et al., 2003; Follows et al., 2007; Sinha et al., 2010; Barton et al., 2010). This becomes a concern when adaptations to environmental changes are to be assessed and thus adaptive potential that at least to some extent mirrors that of the real ocean is crucial. Increased temperatures through climate change are expected to result in shallower mixed layers and hence reduced nutrient availability at low latitudes and increased light exposure at higher latitudes (Sarmiento et al., 2004). Since community composition is heavily influenced by both nutrient availability and temperature, shifts in phytoplankton distributions are to be expected. This is particularly important when taking into account that the efficiency and magnitude of the biological carbon pump is strongly dependent on community composition, especially on the fraction of large, potentially fast sinking types such as diatoms and coccolithophores (Henson et al., 2012).

In this dissertation, different ways of adding realism to phytoplankton models are examined in three model studies: In chapter 2 the effect of varying vs. fixing the N:C ratio in an adaptive single–phytoplankton model at the Bermuda Atlantic Time–Series Study site is examined with respect to the model's predictive power. In chapter 3, the addition of interspecific stoichiometric variation is used to increase long–term diversity

under steady–state conditions in a chemostat and a global model. In chapter 4, the applicability of the previous approach to a non–equilibrium system is investigated.

The remainder of this chapter covers a brief overview of past and present biogeochemical models, with a focus on attempts to resolve phytoplankton complexity via adaptive as well as community–resolving models. With regard to the difficulties of community–resolving models in actually maintaining a community, theories explaining diversity in natural systems are covered in the subsequent section. Next, the role of diversity in natural ecosystems is described briefly, emphasising the benefit of modelling phytoplankton as diverse assemblages, either explicitly or via adaptive dynamics.

1.2 Biogeochemical models

1.2.1 Historical perspective

At present, biogeochemical models are mostly embedded in ocean circulation models (e.g. Follows et al., 2007; Yool et al., 2011; Keller et al., 2012) and consist of a system of coupled ordinary differential equations describing the rate of change of various state variables. Those commonly (but not exclusively) include phytoplankton, zooplankton, detritus and a potentially growth–limiting nutrient, such as nitrogen. This describes the now classical NPZD (nutrient–phytoplankton–zooplankton–detritus) model structure, the origins of which date back to the now famous predator–prey equations by Lotka and Volterra (1926). That model was the first set of coupled differential equations describing population dynamics (Gentleman, 2002). Prey growth was defined by a constant rate, i.e. growth was exponential. Similarly, Fleming (1939) used exponential growth in the first phytoplankton growth model, using basically the same equation for phytoplankton that Lotka and Volterra had used for prey. This use of exponential growth was criticised by Riley, who was convinced that the factor determining the growth rate should be variable: *"The important and difficult problem was that the coefficient of increase in phytoplankton had to be an ecological variable, too"* (Riley, 1984, p. 34). Riley constructed several models of phytoplankton dynamics with increasing complexity and realism; most notably he developed the first coupled physical–biological (Riley and Bumpus, 1946) as well as the first coupled physical–chemical–biological plankton model (Riley, 1946; Gentleman, 2002). Incorporated in the growth rate of the second model were dependencies on light intensity, water transparency and nutrient limitation as well as euphotic zone

depth and vertical turbulence. Later, Riley et al. (1949) developed the first plankton model consisting of coupled ordinary differential equations, namely for nutrients, phytoplankton and zooplankton. This NPZ model also incorporated carnivores, and was able to reproduce observations in different regions of the North Atlantic. The use of this model was limited to rather stable conditions, since computers were not yet available and the equations had to be solved analytically for steady state (Gentleman, 2002).

Those constraints were tackled by John Steele, who used an NPZ model similar to Riley's but with simplified physical equations that allowed him to solve the equations numerically (Steele, 1958). Later, the emerging availability of computers enabled him to replace more parameters with more realistic functions (Steele and Frost, 1977). One prime example is the use of Monod (1949) kinetics for nutrient uptake, which leads to a hyperbolic growth curve as opposed to exponential growth used by Fleming (1939). The Monod function was originally developed for bacterial growth but has since been widely used in biogeochemical models (e.g. Fasham et al., 1990; Schartau and Oschlies, 2003; Gregg et al., 2003; Follows et al., 2007). Another milestone approach in the model by Steele and Frost (1977) was the division of both phytoplankton and herbivorous zooplankton into numerous size classes. Steele and Frost criticised the use of general bulk variables for P and Z and emphasised the necessity of explicitly representing age and species structure of the respective trophic level. Their model's size structure represented different phytoplankton species and different zooplankton age groups, respectively, and size depended on both light and nutrient conditions. In turn, size influenced phytoplankton nutrient uptake, sinking, respiration and grazing rates. The high degree of physiological detail resolved in (Steele and Frost, 1977) allowed for the direct comparison with a local ecosystem, based on the respective local data.

Steele realised that plankton models in general were sensitive to the formulation of the zooplankton equation (Steele, 1976), in particular for the grazing and loss terms. This still applies to many models of pelagic ecosystems (see e.g. Edwards and Yool, 2000; Gentleman and Neuheimer, 2008; Pahlow et al., 2008; Prowe et al., 2012) and presents a large field for model improvements. This study, however, focuses on phytoplankton, therefore in the following, the focus is on equations and parameters governing nutrient–phytoplankton interactions.

Generally, the application of models was mostly limited to specific ocean systems, in earlier as well as in later studies. Regions used for model development and validation include e.g. the North Atlantic (Steele, 1974), the subarctic Pacific (Frost, 1987), the shelf off Oregon (Wroblewski, 1980) or the English Channel (Moloney et al., 1986). A first step towards broader applicability was taken by Evans and Parslow (1985), who tested their NPZ model in both the North Atlantic and the Subarctic Pacific, with the only difference between the two areas being a permanent halocline in the Subarctic Pacific. The model yielded satisfactory fits for both ocean regions, and the underlying assumption that the mixed layer depth is a critical factor in determining plankton dynamics, together with the respective governing equation, was taken up by Fasham et al. (1990). The Fasham et al. (1990) model is a classical NPZD model, which was calibrated using data from the Bermuda Atlantic Time Series Site that was established as part of the US Joint Global Ocean Flux Study (JGOFS) programme in 1988. The model was subsequently coupled to a general circulation model of the North Atlantic (Fasham et al., 1993; Sarmiento et al., 1993).

With the advent of global circulation models, the global applicability of biogeochemical models became a concern. Consequently, for phytoplankton in simple NPZD models, globally valid parameters to create a single all–encompassing phytoplankton had to be determined. Yet phytoplankton communities and parameters obviously differ between ocean regions. Two distinct approaches to address the natural complexity can be distinguished: (1) explicitly simulating various size classes and/or functional types, which results in the need for the respective number of parameter sets for each phytoplankton equation; (2) simulating adaptive potential of a single model phytoplankton, which requires more physiological detail and several equations of state per phytoplankton. Both approaches as well as intermediate solutions are described in the following section, together with their respective strengths and weaknesses.

1.2.2 Tackling phytoplankton complexity in biogeochemical models

The main motivation of increasing modelled complexity is the need for models to be able to assess ecosystem responses to conditions differing from those used to calibrate the model. This applies e.g. to the simulation of ecosystems in ocean regions for which, if at all, only bulk variables such as chlorophyll are available, or to the assessment of possible responses to climate change and the resulting changes in ocean physical proper-

ties. The basic issue was already addressed by Steele (1974), but has since gained much more recognition with the beginning use of biogeochemical models in climate change simulations (Anderson, 2005; Le Quéré et al., 2005; Flynn, 2010).

Simple NPZD models commonly employ the Monod function for growth (Monod, 1949, equation 1.1), and, assuming fixed elemental ratios, this equation also governs nutrient uptake. It assumes a maximum growth rate $\mu_{\max}$ and a monotonic increase in growth with increasing nutrient availability:

$$\mu = \frac{\mu_{\max} N}{K + N} \tag{1.1}$$

where μ is growth rate, N is ambient nutrient concentration and K is the half–saturation constant, i.e. the nutrient concentration at which $\mu_{\max}/2$ is reached. The use of fixed elemental ratios means that a separate equation for nutrient uptake is not necessary since phytoplankton nutrient and carbon differ only by a constant factor. This factor is mostly determined by the Redfield Ratio (Redfield, 1934), such that molar C:N:P = 106:16:1.

The widespread use of the Monod growth function (e.g. Fasham et al., 1990; Schartau and Oschlies, 2003; Le Quéré et al., 2005; Schmittner et al., 2005) has drawn repeated criticism (Aksnes and Egge, 1991; Flynn, 2003, 2010). Most of the criticism regarding the use of the Monod function for nutrient uptake is based on the fact that the half–saturation constant used in the function is not truly a constant, as it varies between phytoplankton types and species, and also within individual cells responding to ambient nutrient and light conditions (Aksnes and Egge, 1991). Essentially the same is true for stoichiometry, which varies considerably in time and space as well as between phytoplankton species(Geider and La Roche, 2002; Redfield, 1934).

Concerns raised with regard to both these major assumptions include the lack of stoichiometric responses to nutrient limitation and growth and vice versa (Flynn, 2010). This is primarily due to the Monod model assuming steady–state conditions for which it was originally developed, but steady state is the exception rather than the rule in the real ocean. Hence, in models used for dynamic simulations, the Monod model is used to simulate the growth and nutrient uptake of a single phytoplankton under often rapidly changing conditions, whereas it was developed in a chemostat and the different values of nutrient concentration vs. growth rate were those of different cultures containing dif-

ferent nutrient concentrations. Dynamic growth of phytoplankton is not accompanied by constant carbon–to–nutrient ratios, and neither is severe nutrient limitation. Consequently, real ocean C:N:P ratios vary in space and time, with values for e.g. C:N ranging from $3\,mol\,C/mol\,N$ under nutrient–replete conditions to $20\,mol\,C/mol\,N$ under nutrient limitation (Goldman et al., 1979). The C:P ratio is even more plastic.

Redfield stoichiometry is frequently used to assess the magnitude of the biological pump, or export production, in models that do not explicitly simulate phytoplankton carbon. The amount of carbon exported to the deep ocean and hence out of contact with the atmosphere is an important tool in assessing future atmospheric CO_2 concentrations. With regard to the previously mentioned weaknesses of assuming constant phytoplankton stoichiometry, calculations of export production based on the respective Redfield ratio of the limiting nutrient (e.g. Laws et al., 2000; Palmer and Totterdell, 2001; Schneider et al., 2008) are likely to lead to errors, possibly drastic ones. Modelled export production is sensitive to modelled primary production (Howard et al., 2006; Schneider et al., 2008), which in turn is determined using the Monod model and Redfield stoichiometry. Another issue regarding the computation of export production is that, based on observations, *"...ecosystem structure (...) is the key factor controlling the efficiency of the biological carbon pump"* (Henson et al., 2012, p.13), emphasising the need for more complexity in pelagic food webs than commonly employed in global models used for climate change assessments.

To date, various models have been developed to increase realism and physiological detail in model formulations of nutrient–phytoplankton interactions. Droop (1973) developed a model using a variable nutrient–to–carbon ratio, which determined growth rate. That is, the higher the cellular nutrient content with respect to carbon, the higher the growth rate, until some maximum is reached. The model includes a minimum nutrient–to–carbon ratio at which growth is zero, which is also termed the subsistence quota. The Droop model is superior to the Monod model in simulating phytoplankton growth of natural lake phytoplankton assemblies in laboratory cultures (Sommer, 1991). Further advances in simulating phytoplankton nutrient uptake and growth independently have been made by e.g. Aksnes and Egge (1991); Geider et al. (1998); Pahlow (2005); Smith and Yamanaka (2007). In the following, the main characteristics of those models are briefly described.

The Aksnes and Egge (1991) model of nutrient uptake is based on the kinetics of nutrient transport across the cell membrane. Transport velocity and hence nutrient uptake rate V depends on the number n and respective area A of nutrient uptake sites, the ion handling time h, the mass transfer coefficient ν and the ambient nutrient concentration N:

$$V = \frac{n\,h^{-1}\,N}{(A\,\nu\,h)^{-1} + N} \tag{1.2}$$

If the Monod equation is expressed in terms of nutrient uptake instead of growth, i.e. μ and $\mu_{\max}$ are replaced by V and $V_{\max}$, respectively, it can be viewed as a special case of the Aksnes and Egge (1991) model, with $K = (A\,\nu\,h)^{-1}$ and $V_{\max} = n\,h^{-1}$. Although the Monod equation was originally considered purely descriptive, its use in phytoplankton models has led to the parameters, especially K, being regarded as physiologically meaningful. The presented reinterpretation of its parameters does indeed allow for that use, although it is to be noted that especially A and n are not constants, but can vary with time (Aksnes and Egge, 1991).

Pahlow (2005) later incorporated the Aksnes and Egge model into an optimisation–based model of phytoplankton growth dependent on nutrients and light. Its basic assumption is that phytoplankton allocates internal resources within the cell so as to maximise growth: nitrogen, assumed to be present primarily in enzymes, is divided first between the cytoplasm and the cell surface, and the latter part is then split up into nutrient uptake enzymes and nutrient assimilation enzymes. Similarly, carbon is divided between the cell, as bulk biomass, and the chloroplast, as chlorophyll enabling growth. Factors governing nutrient uptake and growth are variable and adapt to ambient conditions, e.g. under low-light conditions, chlorophyll synthesis is increased to increase light sensitivity. The model explicitly simulates phytoplankton N, C and chlorophyll, with the latter being regarded as a form of carbon. Comparison of the model with laboratory data of both steady–state and dynamic growth resulted in good fits, showing the model's ability to reproduce non–equilibrium dynamics.

The Pahlow (2005) model was further expanded to include equations for nitrogen, zooplankton, detritus, bacteria and dissolved organic matter and was included in a 1D physical model, which resulted in good agreement with data in the North Atlantic, particularly the lower latitudes (Pahlow et al., 2008). This model is used in chapter 2 for a direct comparison of model performance with regard to fixed vs. optimality–based phytoplankton N:C ratios. It is important to note that, although phytoplankton physiology

adapts to ambient conditions, the time scale on which this is achieved is relatively long, so that Pahlow's model is more of a succession than actual acclimation model (Pahlow et al., 2008), effectively simulating diverse phytoplankton communities in an implicit manner.

As a next step in increasing model complexity, phosphorus limitation was included such that phosphorus content limits nitrogen assimilation, nitrogen content limits chlorophyll synthesis, which in turn limits growth (Pahlow and Oschlies, 2009). Previous models commonly employed Liebig's law of the minimum (von Liebig, 1840) for the simulation of different nutrient limitations, i.e. only one nutrient limits growth at a given point in time. This neglects interactions between nutrients, such as the inhibition of phosphorus limitation on nitrogen assimilation (Pahlow and Oschlies, 2009).

Another extension of the Pahlow (2005) model was done by Smith and Yamanaka (2007), who added other nutrients using the same equations that govern nitrogen dynamics in the original model. Acclimation to the nonlimiting nutrient is governed by the variables determining acclimation to the limiting nutrient, hence cellular nitrogen ratios between the surface and the cytoplasm are the same for all nutrients. The limiting nutrient is determined via Liebig's law of the minimum (von Liebig, 1840).

A different approach to adaptive dynamics was developed earlier by Geider et al. (1998). Their model likewise uses equations of state for phytoplankton carbon, nitrogen and chlorophyll. A classical Monod function for nitrogen uptake is used, albeit with $V_{\max}$ being dependent on the current cell quota of nitrogen to carbon. One major difference to the Pahlow model is that growth is not optimised, but light harvesting is reduced under high light conditions, i.e. chlorophyll synthesis is reduced at high light intensities. In addition, internal nutrient status governs nutrient uptake. The model was later criticised by Armstrong (2006) for not being optimality–based. Armstrong (2006) developed an optimality–based model founded on assumptions similar to those in Pahlow (2005).

Other approaches to adding realism to nutrient–phytoplankton dynamics were used by Flynn (2001), whose model resolved a high degree of physiological detail, but also required considerably more parameters than the models described above.

The complementary approach to increasing complexity in plankton models via physiological detail is the explicit simulation of several species, functional groups or size classes, an idea that was already realised in the model by Steele and Frost (1977). With the use of global circulation models, the number of state variables is limited by computational power, so that at least the early implementations of pelagic ecosystems into global circulation models had to be very restricted in complexity. But with the continuing increase in computer power, resolving for multiple phytoplankton types is no longer much of an issue (Gentleman, 2002). An example of an explicit functional–type–resolving model is that of Gregg et al. (2003), which incorporates diatoms, chlorophytes, cyanobacteria, coccolithophores and zooplankton. The governing equations are comparatively simple, employing the classical combination of Monod and Liebig equations with Redfield stoichiometry, a combination that has been heavily criticised (Flynn, 2010) but is nonetheless commonly applied. A similar approach is used by Sinha et al. (2010), whose model resolves diatoms, coccolithophores, mixed phytoplankton and two zooplankton types and uses the same basic functions for nutrient–phytoplankton interactions.

While PFT–resolving models avoid the need for a single all–encompassing phytoplankton that behaves reasonably well in all ocean areas, as was the case in earlier global modelling studies, the issue still holds for the single functional types. The lack of adaptability within the functional groups neglects the considerable differences that occur even within those groups, not to mention differences within a single species or even cell with regard to nutrient uptake or stoichiometry. An additional issue of PFT–resolving models is that the number of parameters is greatly increased compared to simple NPZD models: parameter number increases approximately with the square of the number of model compartments (Denman, 2003). Those parameters are frequently poorly constrained (Anderson, 2005), and the higher the number of parameters that can be used to tune the model, the higher is the chance of overfitting. This means that a model may well reproduce the characteristics of the model it is fitted to, but fails when compared with independent data (Arhonditsis and Brett, 2004), a problem that is also common in simple NPZD models (Fasham, 1995).

The problem of pre–defining poorly constrained parameters and missing intra–group variability is neatly sidestepped by Follows et al. (2007): A global model is initialised with a large number of phytoplankton types (typically, but not necessarily, 78) distributed among four functional groups, namely diatoms, other large phytoplankton, *Prochlorococ-*

cus–analogs and other small phytoplankton. The nutrient–phytoplankton interactions are determined using Monod and Liebig equations with Redfield stoichiometry, but parameters are assigned randomly from predefined ranges, allowing for the biogeography to emerge in a manner resembling natural selection. Model simulations of chlorophyll and nutrient distributions show good agreement with available data. After initialisation, diversity declines and the distribution of the surviving species or types shows remarkable agreement with observations also with respect to their physiological characteristics (Follows et al., 2007). The model has subsequently been used to assess the coupling of biogeochemistry and ecology through resource competition theory (Dutkiewicz et al., 2009), the mechanisms behind the distribution and coexistence of different phytoplankton types (Barton et al., 2010), the factors controlling nitrogen fixation (Monteiro et al., 2011) and the distribution of different nitrogen fixers (Monteiro et al., 2010) and the effects of increasing detail in the zooplankton compartment (Prowe et al., 2012). In chapter 3, the Dutkiewicz et al. (2009) approach of analysing community composition in the light of resource competition theory (Tilman, 1980) is extended to include variations in phytoplankton stoichiometry.

The Follows et al. (2007) model, through its explicit representation of diversity, exhibits a higher adaptive potential than models with a single species per functional type. However, this is hampered by the fact that frequently one species outcompetes all or most of the others in a given ocean region, a phenomenon also known from other PFT–resolving models (Gregg et al., 2003; Sinha et al., 2010). In the real ocean, the same phenomenon is to be expected from ecological theory, but obviously does not occur, which was first pointed out by Hutchinson: *"The problem that is presented by the phytoplankton is essentially how it is possible for a number of species to coexist in a relatively isotropic or unstructured environment all competing for the same sorts of materials. ... According to the principle of competitive exclusion (Hardin, 1960) ... we should expect that one species alone would outcompete all the others so that in a final equilibrium situation the assemblage would reduce to a population of a single species."* (Hutchinson, 1961, p. 137).

Proposed solutions to the paradox are numerous and diverse and are briefly explained in the following chapter 1.3.2.

1.3 Mechanisms maintaning diversity

The mechanisms maintaining diversity in natural ecosystems have puzzled ecologists for decades and a conclusive explanation is yet to be found. Chesson (2000) summarised proposed theories under two broad concepts: He differentiates between *stabilising* and *equalising* mechanisms. The latter minimise fitness differences between species, the former lead to intraspecific competition being greater than interspecific competition. Both types of mechanisms can be found in plankton communities, but there is no consensus as to which specific mechanism(s) actually explain phytoplankton diversity (Roy and Chattopadhyay, 2007). According to Chesson (2000), stabilising mechanisms can be further divided into fluctuation–dependent and fluctuation–independent processes, whereby it is irrelevant whether fluctuations are generated from within the community, i.e. internally, or imposed from an external source such as changes in environmental conditions. In the following, this distinction is used and examples for each category and subcategory are discussed.

1.3.1 Equalising mechanisms

Equalising mechanisms reduce fitness differences between species. They can promote coexistence through delaying competitive exclusion, but can not prevent it indefinitely (Chesson, 2000). The delay can, however, be long enough that coexistence appears to be permanent (Caswell, 1978). Consider a system that initially consists of a multitude of species exceeding the number of species that could coexist in equilibrium. The time until this equilibrium is reached critically depends on interspecific fitness differences, i.e. the more similar the species, the longer the time until competitive exclusion. Equalising mechanisms prevent the system from reaching equilibrium and hence maintain unstable coexistence. That is, the failure to achieve equilibrium involves the persistence of species that would otherwise go extinct, i.e. they would be competitively excluded. Preventing the occurrence of an equilibrium is all the more likely, the smaller the fitness differences between competing species. Before competitive exclusion is complete, e.g. a generalist predator could eradicate or minimise any differences in biomass that have occurred in the meantime, essentially re–setting the system back to initial or near–initial conditions. Physical external disturbances can have similar effects (see also chapter 4).

1.3.2 Stabilising mechanisms

Fluctuation–independent mechanisms

Stabilising mechanisms punish superior competitors and support inferior ones in a way that allows for indefinite stable coexistence. A classical example is density–dependent predation, i.e. more abundant prey species are consumed at disproportionately high rates. Stable coexistence can also be mediated through bottom–up mechanisms, such as resource partitioning. The key feature of any bottom–up stabilising mechanism is that intraspecific competition must be greater than interspecific competition, which means that a species with a comparatively high growth rate will, through its impact on the environment, reduce its own fitness more than it reduces that of other species. A top–down stabilising mechanism is simpler: superior competitors have a disproportionately higher mortality than inferior ones. Predation or herbivory have been shown to increase coexistence in the next lower trophic level (Chase et al., 2002; Chesson and Kuang, 2008), also specifically for phytoplankton in a biogeochemical model (Prowe et al., 2012). A bottom–up mechanism has been proposed by Tilman (1980) in his resource competition theory, which is an approach developed for steady–state conditions.

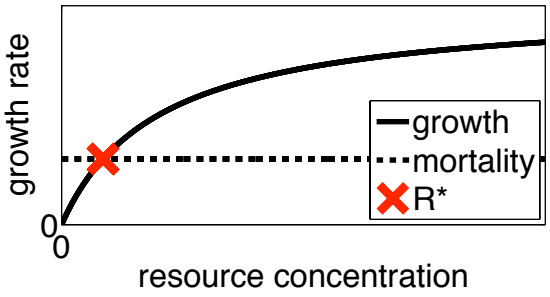

Figure 1.3: The R^* concept (Tilman, 1980): growth increases monotonically with limiting resource concentration while mortality is constant. In equilibrium, growth balances mortality and the resource levels match the species' minimum requirement, R^*.

Resource competition theory relies on two basic concepts: the R^* concept and the existence of trade–offs in parameters determining nutrient limitation. R^* is the minimum concentration of a species' limiting resource at which it can still survive, i.e. where growth balances losses and net growth is hence zero (see figure 1.3). Any phytoplank-

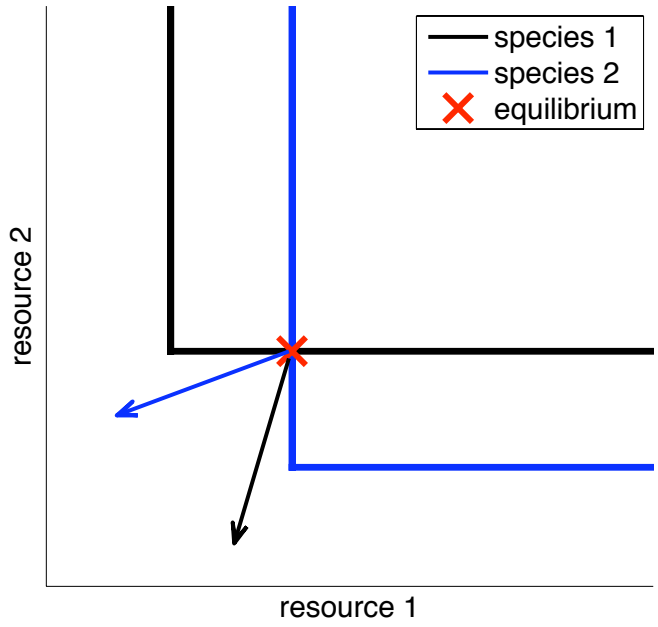

Figure 1.4: Graphical representation of a pair of species parameterised according to resource competition theory (Tilman, 1980): lines represent the species' R^*s for resource 1 and resource 2, respectively. Arrows represent the species' resource consumption vectors. In equilibrium, species 1 is the better competitor for resource 1, and species 2 is the better competitor for resource 2, hence species 1 is limited by resource 2 and species 2 is limited by resource 1. This equilibrium is stable, since each species consumes relatively more of the resource by which it is limited.

ton will, at equilibrium, reduce the resource levels to that concentration. For several species limited by the same resource this means that the species with the lowest R^* can outcompete all others by reducing resource levels too low for its competitors to survive. However, multiple species can coexist if each is limited by a different resource, which requires that each species is the worst competitor for one resource. This is the resource by which the species is limited in equilibrium. For the respective equilibrium to be stable, resource uptake parameters need to be parameterised in a way mirroring the limitation parameters: each species takes up most of the resource that limits its growth at equilibrium. Consequently, by growing and hence taking up resources, it limits its own growth rate more than it limits others. Note that in standard NPZD models that assume

constant elemental composition, nutrient uptake equals growth and hence stoichiometric ratios determine nutrient uptake ratios. The R^* concept is explained in more detail in chapter 3. For a graphical representation, see figure 1.4.

The conditions for the stability of a given equilibrium are commonly ignored in plankton models by parameterising stoichiometry and hence nutrient uptake ratios according to the Redfield Ratio, even if resource competition theory is taken into account with respect to nutrient limitation (see e.g. Dutkiewicz et al., 2009). In chapter 3, nutrient uptake ratios in a chemostat and in a global model are parameterised according to resource competition theory, and the resulting diversity is compared to results from Redfield parameterisation. In chapter 4, it is examined to what extent this approach is valid under disturbance.

Fluctuation–dependent mechanisms

Already Hutchinson (1961) himself, when formulating the now–famous paradox of the plankton, suggested that environmental fluctuations that prevented the occurrence of an equilibrium might prevent competitive exclusion in plankton communities. He did not specify the means of the fluctuation responsible for keeping the system out of equilibrium, and also later studies on the impact of fluctuation on the maintenance of diversity employed a wide range of external fluctuation modes (Gaedeke and Sommer, 1986; Grover, 1988; Sommer, 1995; Flöder and Sommer, 1999; Narwani et al., 2009). A common characteristic of these studies is the focus on temporal variability, yet spatial variability can similarly promote coexistence (Chesson, 2000; Roy and Chattopadhyay, 2007). This study also focuses on temporal variability, since in biogeochemical models small–scale variability is not resolved. Gaedeke and Sommer (1986) and Sommer (1995) used dilution events, i.e. replacing part of the culture with fresh medium, in laboratory cultures as a means of disturbance and their experiments support the intermediate disturbance hypothesis (Grime, 1973; Connell, 1978): disturbance at intermediate levels of either frequency or intensity promotes coexistence, whereas higher or lower intensities lead to competitive exclusion. This hypothesis was likewise supported by Flöder and Sommer (1999), who also applied dilution events, but to natural lake communities.

Dilution as a mode of disturbance or fluctuation imposes two distinct changes on the phytoplankton community: on the one hand nutrient availability is increased ei-

ther through supply from below the mixed layer in the lake or by adding fresh culture medium in the laboratory, stimulating phytoplankton growth. On the other hand, a fraction of each phytoplankton population is removed from the system, essentially imposing mortality. The resulting effects on community structure are (1) reduction of differences in abundances: since species are equally distributed through shaking or stirring before removal, relative removal rates are identical for all species, which amounts to higher absolute removal rates for dominant species; (2) recreating chances at survival for inferior competitors through the input of nutrients. These manipulations alone do not represent a stabilising mechanism *sensu* Chesson. For disturbance to have a stabilising effect on coexistence, relative nonlinearity of competition is required.

Relative nonlinearity of competition is a key ingredient of most externally generated fluctuation–dependent mechanisms. Relative nonlinearity of competition means that species' growth rates respond differently to changing environmental conditions, leading e.g. to the previously superior competitor being weakened and the previously inferior competitor becoming the superior one. This very mechanism is the key component of the intermediate disturbance hypothesis: disturbances induce mortality and create opportunities for growth. Relative nonlinearity of competition is explained through a distinction of "gleaners", i.e. species that are dominant competitors at equilibrium conditions, and "opportunists", essentially colonising species that can achieve high growth rates at high–nutrient conditions but are weak competitors under low–nutrient conditions. Hence, these two types respond differently to disturbance, representing a classical example of relative nonlinearity of competition. Also, between the two types described here, a large range of intermediates is possible, which could further increase diversity.

Grover (1988) used a different approach to disturbance and found that disturbance does not necessarily promote coexistence: Two phytoplankton species were kept in phosphorus–limited culture in chemostats, where dilution was constant. Disturbance was imposed as phosphorus pulses and chemostats receiving no pulses were considered as undisturbed systems. This setting did not support the intermediate disturbance hypothesis but instead supported resource competition theory (Tilman, 1980) irrespective of disturbance. However, the nutrient pulses did slow competitive exclusion. Similar results are attained in model simulations presented in chapter 4. Opposite results with disturbance through nutrient pulses were attained in a model simulation by Ebenhöh (1994) that assumed trade–offs between species: similar species coexisted indefinitely as

long as they formed "a trade–off chain in parameter space" (Ebenhöh, 1994, p. 97).

A simple model using basically the same disturbance mode of intermittent nutrient supply superimposed on a constant dilution rate was used to explain coexistence in a global model (Barton et al., 2010). The global model showed opposite behaviour to those of Grover (1988) and Ebenhöh (1994), i.e. diversity was highest under chemostat–like conditions in the low latitudes, in accordance with observations. This was explained by the coexisting species being competitively equivalent under the given conditions and this hypothesis was verified in a simple model. It did, however, draw criticism with regard to whether it was realistic (Huisman, 2010). Huisman argued that disturbance should increase rather than decrease coexistence. Their different views were based on different assumptions about the nature of coexistence in the model: While Huisman's arguments were based on the intermediate disturbance hypothesis and assumed a gleaner–opportunist tradeoff, Barton and coauthors assessed the coexistence of various gleaners.

High diversity in an undisturbed system was also attained by Narwani et al. (2009). They used dilution at distinct intervals, similar to e.g. Gaedeke and Sommer (1986), as a means of disturbance, but here, unlike in the setup by Grover (1988), the undisturbed system was literally undisturbed: it received no nutrient supply and no additional mortality and was hence a batch culture. The results were strikingly contrary to Grover's: diversity was by far highest in the undisturbed system, which was attributed to internally generated dynamics promoting coexistence.

Internally generated fluctuations, i.e. fluctuations that result from community structure and interactions alone, were shown to increase coexistence in a chemostat (Huisman and Weissing, 1999). A crucial precondition is that competitive abilities of the different species follow a rock–scissors–paper pattern, i.e. species 1 is superior to species 2, species 2 is superior to species 3, which in turn is superior to species 1. The resulting fluctuations can be periodic or chaotic, but biomass levels are comparatively constant. This finding of internally generated fluctuations, which complements findings of increased coexistence under disturbance, has been used to postulate that the paradox of the plankton is essentially solved, since it only applies to equilibrium, which is believed to never occur in the ocean (Scheffer et al., 2003). If that is indeed the case, and disturbance is the predominant mechanism maintaining phytoplankton diversity, models resolving different phytoplankton species or functional groups are missing some fundamental characteristics,

since in models, coexistence is hardly attained. Even seeding a model with a multitude of species per functional type and introducing trade–offs in competitive abilities still does not prevent competitive exclusion, particularly under disturbance (Barton et al., 2010).

1.4 The role of diversity in natural ecosystems

There are two major relations of ecosystem function to diversity: diversity–productivity and diversity–stability (McCann, 2000; Ptacnik et al., 2008; Cardinale et al., 2011). The notion that diversity in ecosystems promotes stability has been a subject of ecological research for decades (see e.g. MacArthur, 1955; Holling, 1973; Steele, 1974; Yodzis, 1981; Tilman and Downing, 1994; Naeem and Li, 1997). There is a general consensus that stability and reliability of ecosystems increase with diversity (Hooper et al., 2005; Cardinale et al., 2011). Stability in this context refers to overall community stability, not to individual species. While individual species' abundances tend to vary more in more diverse communities, overall biomass and ecosystem predictability increase with diversity (Naeem and Li, 1997; McCann, 2000).

The diversity–productivity relationship, i.e. the hypothesis that system productivity is higher in more diverse systems, is supported by data from mostly grassland experiments (Cardinale et al., 2011), but also from phytoplankton communities (Ptacnik et al., 2008; Striebel et al., 2009; Behl et al., 2011). Two distinct effects can lead to increased productivity: (1) the "selection effect", which means that the chance of including a particularly productive species is increased for more diverse assemblies; and (2) the "niche complementarity effect", which encompasses that species use resources differently and thus resource use efficiency is higher in more diverse communities, which also leads to higher overall biomass. Both mechanisms may play a crucial role in maintaining phytoplankton productivity, yet especially under changing conditions, if the selection effect is the dominating mechanism, productivity levels may change significantly. This emphasises the need for modelling phytoplankton as communities instead of all–encompassing non–adaptive species.

1.4.1 Motivation for modelling diversity in biogeochemical models

The call for increased phytoplankton diversity in biogeochemical models is supported by two basic concepts: First, ecosystem function has been shown to depend on diversity (Cardinale et al., 2011). With a single non–adaptive phytoplankton, neither the diversity–productivity relation nor the natural resilience and stability of the pelagic ecosystems are captured, let alone differences between different communities in different biogeographical regions. Consequently, standard NPZD type models already miss important characteristics of ecosystem function in the present ocean.

Second, expected changes in the future ocean add to the number of characteristics missed by simple NPZD models: diversity within a trophic level ensures the function of that trophic level, e.g. carbon fixation through photosynthesis. With biogeochemical models being routinely subjected to climate change scenarios and hence to previously unencountered conditions, changes in community composition and distribution are likely to occur (Hays et al., 2005). If there is only a single non–adaptive model phytoplankton to begin with, those adaptations can not be captured, whereas with multiple species represented, the potential to adequately capture responses to climate change is increased. In addition, if multiple species per functional group are simulated, the "insurance effect" comes into play, i.e. the likelihood that the ecosystem still functions once a species goes extinct is also increased. Ocean ecosystems are expected to undergo significant changes and pressures in the future (Behrenfeld et al., 2006; Boyce et al., 2010), and the corresponding response of the pelagic ecosystem can only be addressed if changes in e.g. community composition are adequately represented. This is not to say that diversity needs to be explicitly resolved; modelling adaptive potential with adaptive models is an implicit way of including diversity, and at least equally viable.

1.5 Thesis overview and author contributions

The main aim of this thesis is to investigate the effect of fixed versus variable phytoplankton stoichiometry on the dynamics of biogeochemical models that resolve for phytoplankton diversity. Two ways of representing phytoplankton diversity are identified: (1) explicitly simulating different phytoplankton types or species and (2) implicitly simulating species succession via adaptive dynamics.

In chapter 2, an adaptive model with originally variable N:C stoichiometry is subjected to an imposed fixed N:C ratio. The two model versions, namely fixed versus variable N:C versions, are tuned to match the observed annual cycle at the Bermuda Atlantic Time–series Study site. Differences in parameter values and model dynamics, especially in predictive power, are subsequently analysed. Chapter 2 is a submitted manuscript with the title "Decoupling phytoplankton N and C improves model predictive power" by L. Göthlich, M. Pahlow and A. Oschlies. L.G., M.P. and A.O. designed the model experiments, M.P. provided the model code and analysing tools. L.G. performed the simulations and L.G., M.P. and A.O. analysed the results. L.G. wrote the paper with comments provided by M.P. and A.O.

In chapter 3, a similar approach is taken to examine the interplay of theoretical ecology and biogeochemical modelling by parameterising a global biogeochemical model according to Tilman's resource competition theory (Tilman, 1980). This model version is compared to a fixed–stoichiometry version with regard to the resulting phytoplankton diversity. The same approach is also used in a simple chemostat model. Chapter 3 is a reprint of the publication *Phytoplankton niche generation by interspecific stoichiometric variation* by L. Göthlich and A. Oschlies (2012), Global Biogeochemical Cycles 26(2). L.G. designed the model experiments, wrote the chemostat model and ran the chemostat simulations. Stephanie Dutkiewicz (MIT, Cambridge, USA) provided the global model code and Friederike Prowe (now at DTU Aqua, National Institute of Aquatic Resources, Denmark) ran the respective simulations. L.G. analysed the results, and L.G. and A.O. wrote the paper.

Since the mechanism maintaining diversity investigated in chapter 3 assumes steady–state conditions, in chapter 4 the validity of the approach under disturbance is investigated. This chapter is a manuscript in preparation by L. Göthlich and A. Oschlies. L.G. and A.O. designed the experiments, L.G. wrote the model code, analysed the output and wrote the paper with comments provided by A.O.

In chapter 5 the main results of chapters 2–4 are summarised and a brief outlook on possible further research is presented.

2 Decoupling phytoplankton N and C improves model predictive power

This chapter is also a submitted manuscript by L. Göthlich, M. Pahlow and A. Oschlies.

Abstract

Marine biogeochemical models commonly include a pelagic ecosystem model, typically comprising nutrient, phytoplankton, zooplankton, detritus (NPZD) compartments or variants thereof. The majority of the incorporated phytoplankton formulations uses fixed stoichiometry in the phytoplankton compartment, coupling carbon (C) and nitrogen (N) cycling via a constant elemental ratio. Yet in the real ocean, phytoplankton stoichiometry can vary in time and space and between species, and has been shown to depend strongly on ambient nutrient concentrations. Here we investigate the impact of accounting for variable stoichiometry on a model's ability to simulate the observed annual cycles of upper-ocean biogeochemical properties at the Bermuda Atlantic Time-series Study (BATS) by comparing two distinctly different model versions: a standard version with dynamically adjusting phytoplankton N:C ratio, and a Redfield version with phytoplankton N:C ratio fixed at the Redfield Ratio. We show that both models can, if tuned appropriately, reproduce the observed seasonal cycles of surface nitrate and vertically integrated chlorophyll similarly well. Yet the fit to independent observational data of primary production and vertical profiles of chlorophyll is substantially improved for dynamically adjusting nitrogen-to-carbon ratios.

2.1 Introduction

Phytoplankton plays a key role in the global carbon cycle by fixing atmospheric CO_2 and thereby providing the basis for all biotically induced carbon export to the deep ocean, predominantly via sinking of organic matter. To quantify this carbon export and address

hypotheses about its controls and sensitivities, biogeochemical models are often used to simulate the cycles of carbon and other climatically relevant elements in the ocean. They typically include a pelagic ecosystem model consisting of state variables for nutrient, phytoplankton, zooplankton and detritus (NPZD) compartments (e.g. Schmittner et al., 2005), sometimes in several subcategories, e.g., different phytoplankton functional groups (Follows et al., 2007; Sinha et al., 2010). An important aspect of NPZD models is the conversion of inorganic nutrients into biomass via photosynthesis and nutrient uptake by phytoplankton. The way in which these processes are modelled critically depends on whether or not phytoplankton elemental composition is flexible or fixed. A common procedure is to fix phytoplankton stoichiometry at a constant ratio (commonly the Redfield Ratio, Redfield, 1934). This assumes that nutrient uptake and growth are tightly coupled processes which, in reality, they are not (Geider and La Roche, 2002).

To systematically investigate the impacts of variable versus fixed nitrogen to carbon (N:C) ratios and the respective differences in phytoplankton nutrient uptake and growth on marine biogeochemistry, two phytoplankton formulations were examined in the framework of an existing NPZD (nutrient-phytoplankton-zooplankton-detritus) model (Pahlow et al., 2008) and applied to the BATS site (Bermuda Atlantic Time-series Study, Steinberg et al., 2001). The plankton model treats biomass as carbon (C) and allows decoupling of carbon and nitrogen (N) dynamics for phytoplankton and detritus. It contains an optimality-based formulation of phytoplankton growth which, at each model time step, allocates cellular C and N among nutrient and light utilisation machineries such that instantaneous phytoplankton growth is maximised. This model (hereafter called the standard version) has been shown earlier to allow for a good simulation of the BATS system that, in many aspects (in particular realistic levels of high primary production in summer) appeared more realistic than the results of earlier models (see e.g. Pahlow et al., 2008).

The present study investigates to what extent this apparent improvement over previous model studies (Doney et al., 1996; Fasham et al., 1990; Schartau and Oschlies, 2003) can be attributed to the dynamic decoupling of N and C cycles. To this extent, the standard version will be compared against a fixed N:C version of the same model (hereafter called the Redfield version). Besides showing differences in stoichiometry, the two model versions also differ markedly in their simulated ecosystems' ability to use ambient N: Under low ambient N, the standard model version allows for the assimilation of about

three times as much biomass (C) per unit N and, hence, N uptake at low ambient N is considerably more efficient compared to the Redfield version.

In the following, both standard and Redfield model configurations are fitted to observations of surface nitrate and vertically integrated chlorophyll at BATS. The differences in goodness-of-fit and estimated parameter values are discussed, before the predictive capability of both models is evaluated against independent data of primary production and depth profiles of chlorophyll.

2.2 Ocean station BATS

The Bermuda Atlantic Time-series Study (BATS) site is situated at 31°N, 64°W in the western North Atlantic subtropical gyre, 82 km southeast of Bermuda, and was established as a time-series station during the US Joint Global Ocean Flux Study (JGOFS) programme in 1988. Sampling was conducted on a biweekly to monthly basis, allowing for resolution of major seasonal patterns as well as interannual variability. The annual cycle at BATS is characterised by deep winter mixing down to 200–300 m, followed by strong stratification in spring and summer, with mixed layer depths as shallow as 20 m (Steinberg et al., 2001). Winter mixing injects nutrients into the euphotic zone, stimulating an annually recurring phytoplankton bloom in late winter/early spring (January–March). During summer, nitrate in the upper mixed layer is depleted below the detection limit, and a deep chlorophyll maximum forms below the mixed layer at depths between about 50–100 m (Steinberg et al., 2001). The ecosystem at BATS is generally considered oligotrophic with surface nitrate values ranging from 0 to $\approx 1\,\mu\mathrm{mol\,kg^{-1}}$, phosphate mostly below $0.05\,\mu\mathrm{mol\,kg^{-1}}$ and chlorophyll reaching $\approx 0.4\,\mu\mathrm{g\,kg^{-1}}$ in the deep chlorophyll maximum (Michaels et al., 1994). Hence, the system is dominated by the microbial loop, and both bacteria and (micro-) zooplankton play an important role in the carbon and nutrient cycles (Steinberg et al., 2001).

2.3 Model

The biogeochemical model was coupled off-line to the three-dimensional North Atlantic circulation model of Oschlies and Garçon (1999) and applied as described in Schartau

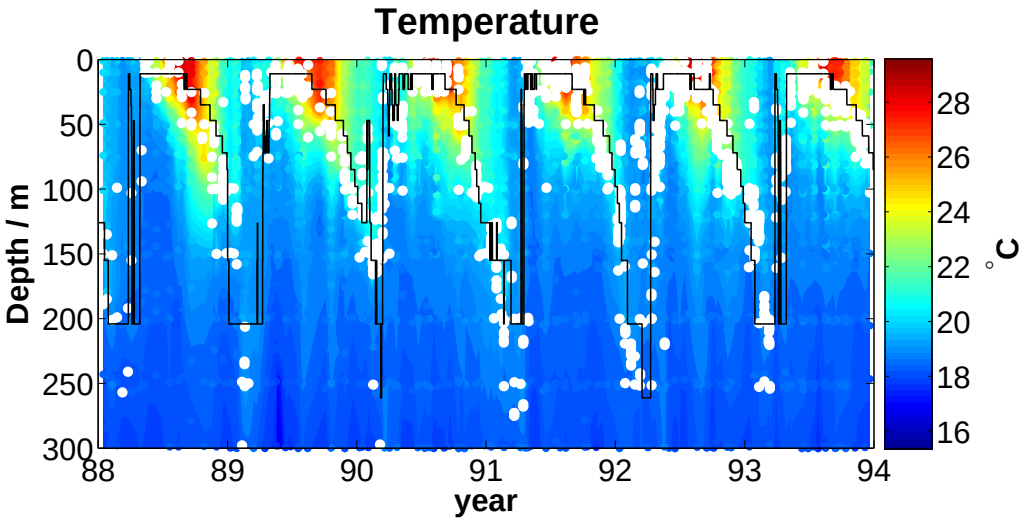

Figure 2.1: Temperature (contours) and modelled (black line) and observed (white dots) mixed layer depth, defined as the deepest point at which the density difference to the surface is less than 0.1 kg/m^3, at BATS.

and Oschlies (2003). The model domain consists of 27 depth levels with a top layer thickness of 11 m, and a closed bottom boundary at the sea floor. The circulation model was forced with daily mean reanalysis data from the European Centre of Medium Range Weather Forecast (ECMWF) for the years 1988–1993. Fig. 2.1 shows observed and modelled mixed layer depths (MLD) at BATS. MLD was calculated as the deepest point at which the density difference to the surface is less than $0.1\,kg\,m^{-3}$. Maximum modelled MLD was ≈ 260 m, spanning 13 depth levels.

The biogeochemical model (Fig. 2.2) is a slightly reduced version (i.e. without bacteria and dissolved organic matter) of the adaptive NPZD-type model developed by Pahlow et al. (2008). The model is based on nitrogen (N) and carbon (C), with state variables for phytoplankton N, C and chlorophyll, as well as for zooplankton C, dissolved inorganic nitrogen (DIN) and detritus N and C. Phytoplankton takes up DIN and produces biomass via carbon fixation during photosynthesis. In addition, the dynamic optimal temperature for phytoplankton growth was replaced by a simple temperature factor for phytoplankton, calculated as $1.066^{(T-27^\circ\mathrm{C})}$ (Eppley, 1972) in the current study.

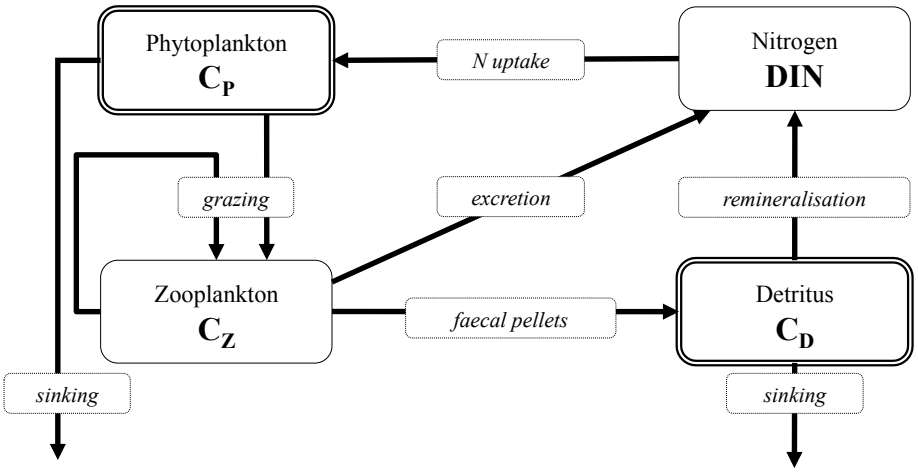

Figure 2.2: Model structure: boxes with double lines indicate state variables with both N and C modelled in the "standard" configuration (i.e. variable N:C ratios); arrows indicate elemental fluxes.

2.3.1 Phytoplankton

In our standard model configuration, phytoplankton C, N and chlorophyll dynamically adjust to ambient conditions so as to maximise instantaneous growth rate (Pahlow, 2005). Both C and N are optimally allocated to allow for efficient utilisation of light and nutrients (see table 2.1 for symbols used in the text). The following is a brief description of the allocation mechanisms, (see Pahlow, 2005, for details): Cellular N is split up between a variable fraction used for photosynthesis ($Q - Q_0$), and a constant fraction (Q_0) used to acquire DIN. The fraction Q_0 is then split up between the protoplast and nutrient uptake sites at the cell surface, allowing for optimal allocation within Q_0 to maximise N uptake as proposed by Aksnes and Egge (1991): N in the nutrient uptake enzymes at the cell surface determines the cell's affinity for DIN. N in the protoplast is contained in enzymes used for nutrient assimilation and determines the maximum DIN uptake rate. The two N fractions in the protoplast and at the cell surface are adjusted to maximise nutrient uptake: Affinity is increased at low, maximum uptake rate is increased at high ambient DIN concentrations. Photoacclimation allocates photosynthetically fixed C to either chlorophyll or the rest of the cell (i.e., as biomass or used for compounds that fuel respiration) in order to maximise net instantaneous energy generation. In our simplified Redfield version, N:C dynamics and the corresponding optimal allocation of intracellular

N are disabled and a fixed (Redfield) N:C ratio is employed. DIN uptake is described by optimal uptake kinetics (Pahlow, 2005), which, in the Redfield model, depends solely on ambient DIN.

2.3.2 Zooplankton

Zooplankton ingests phytoplankton and zooplankton and excretes DIN and faecal pellets, which are the only source of detritus in this model. Detritus sinks at a constant speed, and is remineralised to DIN and CO_2 at a constant rate. Grazing results in ingestion of both C and N, in variable ratios due to different N:C ratios between model compartments, but N and C are assimilated into zooplankton biomass at a constant zooplankton N:C ratio. This constant zooplankton N:C ratio is maintained through a variable N:C ratio of the excreted faecal pellets, which accounts for the difference between ingested and assimilated N:C ratios. To aid conceptual simplicity, a few further changes were applied with respect to the original Pahlow et al. (2008) model: Zooplankton feeding on detritus was removed and grazing preferences were made proportional to the respective prey concentration, thus treating herbivory and carnivory equally. In the original model, grazing on detritus is allowed, grazing preferences are dynamic property state variables (Pahlow et al., 2008). Ingestion (grazing, G) is described by a modified form of the function of Peters (1994), an empirical representation of microzooplankton grazing that includes an exponential function of temperature (T) and different powers of biomass concentration (C) and size (m) of prey and predator:

$$G = \mathrm{e}^{-C_0/C_{\mathrm{prey}}} f_I m_{\mathrm{prey}}^{0.167} m_{\mathrm{pred}}^{-0.253} C_{\mathrm{prey}}^{0.489} C_{\mathrm{pred}}^{-0.27} \mathrm{e}^{0.064(T-27^\circ\mathrm{C})} \tag{2.1}$$

For definitions and units of variables and parameters, see table 2.1. This empirically determined shape of grazing as a function of prey concentration is rather atypical for grazing functions used in current models, since it starts extremely steeply at zero prey concentration and shows no saturating behaviour. The grazing threshold (C_0) in Eq. 2.1 is not part of the original equation and was introduced to ensure numerical stability (Pahlow et al., 2008). The main effect of the threshold is that the steep initial increase of the grazing function is shifted slightly to finite prey concentrations, which effectively creates a refuge at very low prey concentrations.

Table 2.1: Units and definitions of variables and parameters; ranges and best fit parameter values

symbol	unit	definition	range	standard	Redfield
		Bulk Variables			
C_D	$\mathrm{gC\,m^{-3}}$	detritus carbon concentration			
C_P	$\mathrm{gC\,m^{-3}}$	phytoplankton carbon concentration			
C_Z	$\mathrm{gC\,m^{-3}}$	zooplankton carbon concentration			
N_D	$\mathrm{gN\,m^{-3}}$	detritus nitrogen concentration			
N_P	$\mathrm{gN\,m^{-3}}$	phytoplankton nitrogen concentration			
N_i	$\mathrm{gN\,m^{-3}}$	ambient DIN concentration			
		Other variables			
α	$\mathrm{m^2 gC(\mu E\ gChl)^{-1}}$	phytoplankton light absorption coefficient			
A	$\mathrm{m^{-3}(gC\,d)^{-1}}$	phytoplankton DIN affinity			
μ_P	$\mathrm{d^{-1}}$	phytoplankton growth rate			
R_P^C	$\mathrm{d^{-1}}$	phytoplankton respiration rate			
$\hat{\theta}^C$	$\mathrm{gChl\,gC^{-1}}$	chloroplast Chl:C ratio			
V_N^C	$\mathrm{gN\,gC^{-1}\,d^{-1}}$	phytoplankton N uptake			
V_max^C	$\mathrm{gN\,gC^{-1}\,d^{-1}}$	phytoplankton max. N uptake per unit biomass			
C_pred	$\mathrm{gC\,m^{-3}}$	predator concentration			
C_prey	$\mathrm{gC\,m^{-3}}$	food concentration			
E_Z^C	1	zooplankton assimilation efficiency			
f_Z^d	1	dissolved fraction of zooplankton excretion			
G_x	$\mathrm{d^{-1}}$	grazing rate on group x			
m_prey	$\mathrm{pgC\,organism^{-1}}$	prey size			
m_pred	$\mathrm{pgC\,organism^{-1}}$	predator size			
ψ_x	1	zooplankton food preference for group x			
Q_D	$\mathrm{mol\,N\,mol\,C^{-1}}$	detritus N:C ratio			
R_Z^C	$\mathrm{d^{-1}}$	zooplankton respiration rate			
X_Z^N	$\mathrm{gN\,m^{-3}\,d^{-1}}$	zooplankton N excretion			
I	$\mu\mathrm{E\ m^{-2}\,d^{-1}}$	irradiance			
T	°C	ambient temperature			

continued on next page

Table 2.1: Units and definitions of variables and parameters; ranges and best fit parameter values – continued

Symbol	Unit	Definition	range			standard	Redfield
		Phytoplankton parameters					
α_0	$10^{-5}\,\mathrm{m^2 gC}(\mu\mathrm{E\ gChl})^{-1}$	phytoplankton reference light absorption coeff.	0.3	–	2	1.5	0.33
A_0	$\mathrm{m^3\,(gC\,d^{-1})}$	phytoplankton max. affinity for DIN	5	–	150	90	47.85
μ^*	$\mathrm{d^{-1}}$	phytoplankton max. metabolic rate at 27°C	1	–	20	4.5	6.65
Q_P	$\mathrm{mol\,N\,mol\,C^{-1}}$	phytoplankton N:C ratio		0.15		variable	0.15
Q_0	$\mathrm{mol\,N\,mol\,C^{-1}}$	phytoplankton subsistence N:C ratio	0.02	–	0.08	0.046	–
R^M	$\mathrm{d^{-1}}$	phytoplankton maintenance respiration rate		0.0017		0.0017	0.0017
ξ_0	$\mathrm{gC\,gChl^{-1}}$	cost of chlorophyll synthesis	5	–	20	7.14	15.84
		Zooplankton and detritus parameters					
C_0	$\mathrm{gC\,m^{-3}}$	zooplankton grazing threshold		0.01		0.01	0.01
f_I	$\mathrm{m^3\,gC^{-1}d^{-1}}$	zooplankton reference filtering rate factor	1	–	15	5.51	1.67
E_Z^N	1	zooplankton max. N assimilation efficiency	0.7	–	0.95	0.76	0.75
D_D	$\mathrm{d^{-1}}$	detritus disintegration rate	0.05	–	0.1	0.09	0.07
v_D^s	$\mathrm{m\,d^{-1}}$	detritus sinking velocity	3	–	10	5.61	9.58
f_0^d	1	min. dissolved fraction of zooplankton excretion	0.1	–	0.7	0.36	0.16
R_Z^m	$\mathrm{d^{-1}}$	zooplankton base respiration rate	0.03	–	0.1	0.05	0.07

2.3.3 Parameter estimation

Parameters were estimated in a step-wise manner, adjusting first the zooplankton and detritus parameters and subsequently the phytoplankton parameters. For each model version, starting from the initial parameter set (taken from the 'constant efficiency' model version of Pahlow et al., 2008) 60 new parameter sets were generated by a Monte Carlo routine, with the zooplankton and detritus parameters generated from random uniform distributions within biologically reasonable ranges for each parameter (see Table 2.1 for parameters used to fit the model to the observations). This resulted in a good fit of the standard model version to the observed annual cycle of surface DIN and vertically integrated Chlorophyll, but not of the Redfield version. Thus, phytoplankton parameters were adjusted in the same way, using the best of the Redfield runs as a template and changing only the phytoplankton parameters in 60 sets generated from random uniform distributions within biologically reasonable ranges. This amounted to a total of 180 model runs. A best fit was chosen for each model version, based on visual inspection of wether or not surface nitrate was used up in summer and if so, at what time the depletion occurred, indicating the end of the phytoplankton bloom. Additionally, winter peak values of nitrate and their timing were taken into account, as was the annual cycle of vertically integrated chlorophyll.

2.4 Results

Both model versions reproduce the annual cycles of chlorophyll and dissolved inorganic nitrogen at BATS (Fig. 2.3): the annual DIN peak in winter fits the observed values in both timing and extent, as well as the annual late winter/early spring phytoplankton bloom terminated by total depletion of DIN. This depletion occurs earlier and more abruptly in the standard version (Fig. 2.3b) compared with the Redfield version (Fig. 2.3d), and hence is in better agreement with the observations, but otherwise both model versions reproduce the data similarly well.

In contrast, the modelled time-averaged depth profiles show considerable differences in the model versions' respective ability to reproduce independent data to which the model was not fitted: the Redfield version fails to reproduce the deep primary production (Fig. 2.4a). This essentially restricts primary production to the upper 30m, whereas the standard version, while still underestimating primary production especially

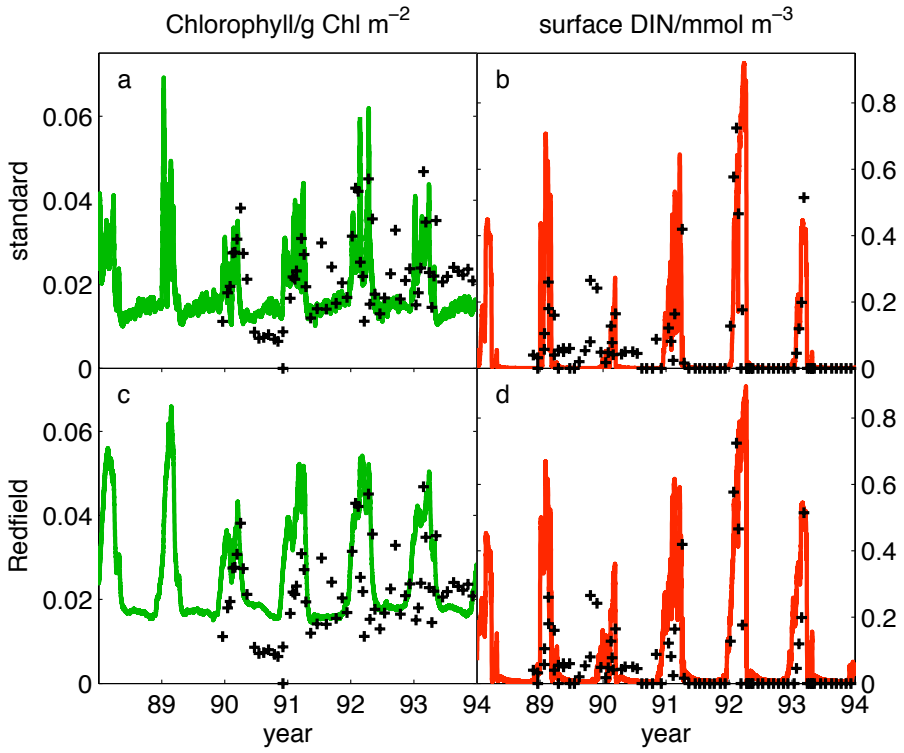

Figure 2.3: Predicted annual cycle at BATS for the standard and Redfield model versions. left: vertically integrated chlorophyll, right: surface dissolved inorganic nitrogen. Data from http://bats.bios.edu/ are shown as crosses.

at the surface, qualitatively reproduces the observed depth profile. The modelled chlorophyll profiles (Fig. 2.4b) highlight another deficiency of the Redfield version: the deep chlorophyll maximum (DCM) is not reproduced at all, while surface chlorophyll is overestimated by a factor of 2. The DCM is reproduced by the standard version, although its depth is underestimated.

2.5 Discussion

Compared to higher latitudes, phytoplankton standing stocks at BATS are persistently small throughout the year. Still, summer primary production and chlorophyll values are relatively high for the prevailing oligotrophic conditions in this region (Michaels et al.,

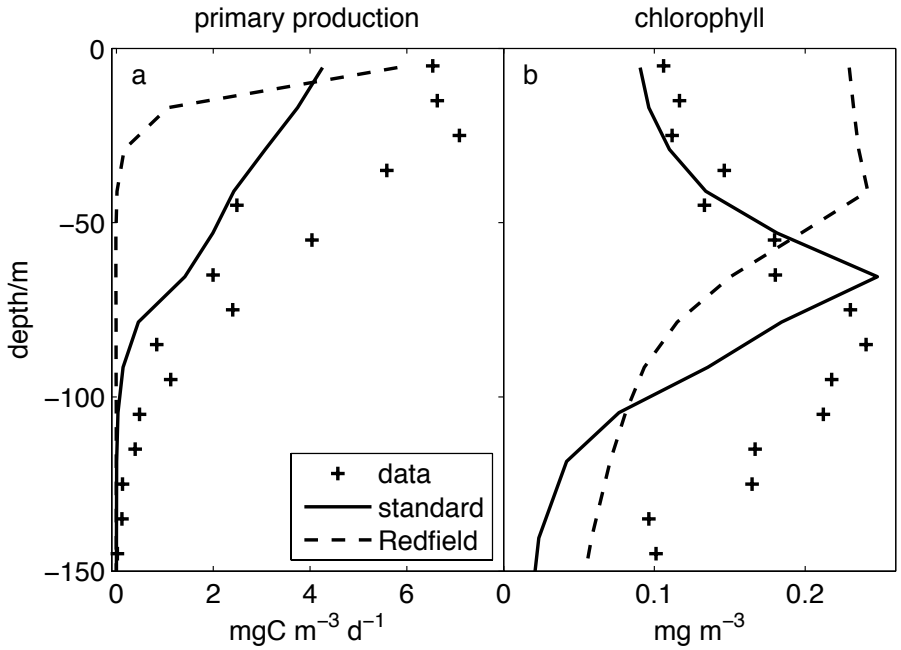

Figure 2.4: Averaged observed and modelled profiles of (a) primary production and (b) chlorophyll at BATS

1994). This requires efficient nutrient uptake and recycling and has proven difficult to capture in previous model studies (Doney et al., 1996; Fasham et al., 1990; Schartau and Oschlies, 2003). Results of a model with decoupled N and C cycles suggested a relatively good simulation of the BATS system (see e.g. Pahlow et al., 2008). The present study investigates to what extent this apparent improvement can be related to the dynamic decoupling of N and C cycles. To this extent, a dynamic N:C model is directly compared to its fixed-N:C counterpart, i.e. the same model with only the N:C dynamics switched off. This allows for systematic investigation of their respective ability to reproduce the BATS data.

While both model versions are able to capture the dynamics of the surface chlorophyll and DIN annual cycles at BATS (Fig. 2.3), the parameter values used to achieve a good fit differ considerably between the two versions (Table 2.1). Since the model is very sensitive to the zooplankton compartment (Pahlow et al., 2008), the zooplankton parameters were optimised first. The most obvious difference occurs in parameter f_I,

the factor governing overall grazing activity, which is more than 3 times smaller in the Redfield version. Other parameters showing significant differences are the detritus sinking velocity v_D^s, which is almost twice as fast in the Redfield version, and the minimum dissolved fraction of zooplankton excretion f_0^d, which is more than 2 times smaller in the Redfield version.

High C:N ratios under nutrient-limited and light-replete conditions, which commonly occur at BATS during summer, can be attained in the standard version, but not in the Redfield version with its fixed C:N stoichiometry. Since N uptake is proportional to biomass, N uptake at low ambient DIN is considerably more efficient in the standard than in the Redfield version. Consequently, in our standard phytoplankton model, phytoplankton can take up nutrients at very low ambient concentrations and efficiently convert them into biomass, hence comparatively high grazing pressure is needed to keep modelled phytoplankton biomass low. The rather strong grazing control at low food concentration, owing to the steep initial slope of the grazing formulation, balances the efficient nutrient utilisation of the standard phytoplankton model. Strong grazing control, on the other hand, can potentially keep phytoplankton concentration so low that a significant amount of DIN remains unutilised, as was frequently observed in Redfield model runs with higher values for f_I (data not shown).

In the Redfield model version, phytoplankton growth is proportional to nutrient uptake and hence not as flexible in responding to variations in nutrient supply as in the standard version. On the one hand, this requires a low enough grazing pressure in order to maintain a sufficiently large phytoplankton standing stock to utilise all ambient DIN, especially in summer. On the other hand, this phytoplankton standing stock, when using the same parameters as in the standard version, is considerably overestimating BATS chlorophyll data by a factor of about 2 (not shown). In summary, optimising only the zooplankton and detritus parameters resulted in a satisfactory fit for the DIN data, but chlorophyll was overestimated.

Consequently, the most important phytoplankton parameters in terms of model sensitivity were optimised in another Monte-Carlo sampling, namely the light absorption coefficient α_0, the maximum DIN affinity A_0, the potential photosynthetic rate μ_*, and the cost of chlorophyll synthesis ξ_0. The best fit resulting from this second optimisation to observations of surface DIN and vertically integrated chlorophyll is comparable to

the best fit of the standard model. Parameter values showing considerable differences between the model versions are those determining chlorophyll dynamics, α_0 and ξ_0. The lower α_0 leads to reduced C assimilation, while the higher ξ_0 results in less chlorophyll synthesized per unit biomass. Hence, the phytoplankton Chl:C ratio is reduced compared to the standard version.

The importance of the chlorophyll parameters can be attributed to the fact that the variability of the Chl:C ratio is reduced by $\pm 50\%$ in the Redfield version. This is due to half of the Chl:C variability in the standard model version being attributable to the variability in N:C since chlorophyll synthesis is proportional to the N:C ratio (for details see Pahlow, 2005). With N:C fixed at the Redfield ratio, Chl:C is less variable and on average higher than in the standard version. The parameter values of the Redfield run compensate for these differences and even reduce average Chl:C to values lower than Chl:C in the standard version ($\sim 0.015\,\mathrm{gChl\,gC^{-1}}$ in the Redfield version vs. $\sim 0.02\,\mathrm{gChl\,gC^{-1}}$ in the standard version), which balances the differences in phytoplankton standing stocks. Although the two models calibrated against surface DIN and vertically integrated chlorophyll data simulate very similar chlorophyll values, phytoplankton standing stocks (measured in carbon) differ significantly between the two, being $\geq 50\%$ higher in the Redfield version. For phytoplankton N, the difference is even more pronounced, owing to the fixed N:C quota at $0.15\,\mathrm{gN\,gC^{-1}}$ in the Redfield version, while the N:C quota in the standard version regularly reaches values as low as $0.09\,\mathrm{gN\,gC^{-1}}$.

Yet the most obvious difference between the two model versions is their respective ability to reproduce independent observations that were not used to calibrate the model. This was tested by confronting the two calibrated models with time-averaged depth profiles of chlorophyll and primary production. While the standard version qualitatively reproduces both chlorophyll and primary production values relatively well, the Redfield version fails to capture essential characteristics of either dataset (Fig. 2.4). Thus, the different parameter combinations calibrated to achieve a similar goodness-of-fit to key data characterising the BATS annual cycle do not lead to the same predictive power of the respective model. The standard model with its variable N:C ratio and the corresponding high growth efficiency is apparently better suited to reproduce independent observations it has not been fitted to, compared to the Redfield version of the otherwise identical model. This demonstrates that refinement in phytoplankton formulations with regard to

nutrient and carbon dynamics can lead to significant improvements in model predictive power compared to fixed N:C models. Predictive power is especially crucial when one attempts to simulate future biogeochemical responses to increased sea surface temperature and elevated CO_2 with models tuned to reproduce past and present observations. Models developed for this purpose commonly employ phytoplankton stoichiometry fixed at the Redfield Ratio (Redfield, 1934; Schmittner et al., 2005; Follows et al., 2007; Sinha et al., 2010).

While our Redfield model allows for a realistic annual DIN and chlorophyll cycle at BATS, fixing the N:C ratio does not reflect the actual situation in the ocean where the Redfield Ratio is, if at all, only valid in an average sense. Individual species' N:C stoichiometries tend to differ from one another, and even those of a single species can vary in time and space (Geider and La Roche, 2002; Anderson and Pondaven, 2003; Klausmeier et al., 2004), with the strongest deviations expected for strong nutrient limitation (Pahlow and Oschlies, 2009). Using the Redfield Ratio can significantly impair model performance, especially under severe nutrient limitation (Flynn, 2010), which frequently occurs at BATS. We demonstrate here that it can also lead to reduced predictive power compared to a flexible-N:C model.

2.6 Summary and conclusion

Two plankton model versions, derived from the same original model (Pahlow et al., 2008), a common Redfield-type fixed N:C version and an optimality-based flexible N:C version, were compared with respect to their ability to reproduce the annual cycle of surface DIN and chlorophyll at the BATS site. While both model versions can be fitted to the annual cycle data, the respective best fits differ markedly in their ability to reproduce independent observations not used to calibrate the model: the optimality-based model qualitatively reproduces time-averaged depth profiles of chlorophyll and primary production, whereas the Redfield version fails to capture essential characteristics of either dataset.

We conclude that the Redfield version lacks the flexibility to capture the nutrient-limited dynamics of the BATS site, which is attributed to the Redfield Ratio being valid only in an average sense, which does not reflect the N:C dynamics in the ocean. The

variable N:C model version, however, qualitatively reproduces the observations it has not been fitted to, hence its predictive power is significantly higher than that of the Redfield version. With models like these used to simulate the future ocean, predictive power is increasingly crucial. Thus, models employing the Redfield Ratio may not exhibit sufficient predictive power for this purpose and replacing them with more flexible models should be taken into consideration.

Acknowledgements

L.G. acknowledges funding by the Deutsche Forschungsgemeinschaft (DFG) via SFB 754.

2.7 Appendix: Model equations

The differential equations for material state variables are of the form:

$$\frac{\mathrm{d}Y}{\mathrm{d}t} = p^Y - c^Y + D^Y \tag{2.2}$$

where p^Y is (net) production of state variable Y, c^Y is consumption of Y and D^Y is the rate of change in Y due to advection and diffusion. In the following, p^Y and c^Y is shown for each of the model's state variables, respectively. In addition, the phytoplankton equations that exhibit differences between the two model versions are included. For further detail, see Pahlow et al. (2008).

Phytoplankton

In the following, the core model equations are given, for both the standard and Redfield model versions. Variables and parameters are defined in table 2.1. Nutrient uptake is modified from Pahlow (2005):

$$V_N^C = \frac{1}{{V_{\max}^C}^{-1} + (A\,N_\mathrm{i})^{-1}} \tag{2.3}$$

where $V^C_{\max}$ is max. nutrient uptake per unit biomass, A is phytoplankton affinity for DIN and N_i is the ambient DIN concentration. V^C_N is temperature dependent because $V^C_{\max}$ and A are functions of μ^* (the maximum metabolic rate). Phytoplankton N uptake is the same in both model versions:

$$p^{N_P} = \left(\frac{V^C_N}{Q_P} - 1.066^{(T-27°\mathrm{C})}\, R_M\right) N_P \tag{2.4}$$

where V^C_N is nutrient uptake, Q_P is phytoplankton N:C ratio, T is temperature and R_M is phytoplankton maintenance respiration rate. Net phytoplankton (C) production in the standard model version is defined by:

$$p^{C_P} = \left(\mu_P - R^C_P\right) C_P \tag{2.5}$$

where μ_P and R^C_P are rates of gross growth and respiration. Phytoplankton gross growth in the standard model version depends on the phytoplankton N:C quota:

$$\mu_P = 1.066^{(T-27°\mathrm{C})}\, \mu^* \frac{Q_P - Q_0}{Q_P} \left(1 - \mathrm{e}^{-\alpha\, I \frac{\hat{\theta}^C}{\mu^*}}\right) \tag{2.6}$$

where T is temperature, μ^* is the maximum metabolic rate, Q_p is the phytoplankton N:C ratio, Q_0 the subsistence N:C ratio, α is the phytoplankton light absorption coefficient, I is irradiance, $\hat{\theta}^C$ is the chloroplast Chl:C ratio and μ^* is the maximum metabolic rate. In contrast, in the Redfield model version, phytoplankton gross growth is determined by N uptake, unless phytoplankton is light-limited, in which case equation 2.6 applies:

$$\mu_P = \min\left(\frac{p^{N_P}}{N_P},\ 1.066^{(T-27°\mathrm{C})}\, \mu^* \frac{Q_P - Q_0}{Q_P} \left(1 - \mathrm{e}^{-\alpha\, I \frac{\hat{\theta}^C}{\mu^*}}\right)\right) \tag{2.7}$$

where p^{N_P} is phytoplankton N uptake and N_P is phytoplankton N concentration. Phytoplankton consumption is due to grazing:

$$c^{C_P} = \psi_P\, G_P\, C_Z \tag{2.8}$$

where C_Z is zooplankton (C) concentration, ψ_P is the grazer's preference for phytoplankton and G_P is net (C) ingestion of phytoplankton through grazing as defined in equation 2.1. The model uses different sizes for both phytoplankton and zooplankton which are reflected in the actual ingestion rates. These are omitted here for simplicity, for a detailed description see Pahlow et al. (2008).

(2.9)

DIN, zooplankton, detritus

Other model compartments do not exhibit differences between the standard and Redfield model versions. DIN production and loss rates are as follows:

$$p^{N_\mathrm{i}} = R_M \, 1.066^{(T-27^\circ\mathrm{C})} N_P + X_Z^N \, f_Z^d + D_D \, N_D \tag{2.10}$$

$$c^{N_\mathrm{i}} = V_N^C \, C_P \tag{2.11}$$

where R_M is phytoplankton metabolic N loss rate, T is temperature, N_P is phytoplankton N concentration, X_Z^N is zooplankton N excretion, f_Z^d is the dissolved fraction of zooplankton excretion, D_D is the detritus disintegration rate, N_D is detritus N concentration, V_N^C is phytoplankton N uptake and C_P is phytoplankton C concentration.

Zooplankton net production is described as follows:

$$p^{C_Z} = \left(E_Z^C \, G^C - R_Z^C\right) C_Z \tag{2.12}$$

where E_Z^C is zooplankton assimilation efficiency, G^C is zooplankton net ingestion rate, R_Z^C is zooplankton respiration and C_Z is zooplankton C concentration. Zooplankton itself is explicitly included in the food (carnivory), leading to the zooplankton loss term:

$$c^{C_Z} = \psi_Z \, G_Z \, C_Z \tag{2.13}$$

where C_Z is zooplankton (C) concentration, ψ_Z is the grazer's preference for zooplankton and G_Z is net (C) ingestion of zooplankton through grazing as defined in equation 2.1.

Detritus net production is described as follows:

$$p^{C_D} = X_Z^C \left(1 - f_Z^d\right) - D_D \, C_D \tag{2.14}$$

$$p^{N_D} = X_Z^N \left(1 - f_Z^d\right) - D_D \, N_D \tag{2.15}$$

where X_Z^C and X_Z^N are C and N excretion by zooplankton, f_Z^d is the dissolved fraction of zooplankton excretion, D_D is the detritus disintegration rate and C_D andN_D are detritus C and N concentrations, respectively. Detritus losses occur through grazing:

$$c^{C_D} = \psi_D \, G_D \, C_Z \tag{2.16}$$

$$c^{N_D} = c^{C_D} \, Q_D \tag{2.17}$$

$$\tag{2.18}$$

where C_Z is zooplankton (C) concentration, ψ_D is the grazer's preference for detritus, G_D is net (C) ingestion of phytoplankton through grazing as defined in equation 2.1 and Q_D is the detritus N:C ratio.

3 Phytoplankton niche generation by interspecific stoichiometric variation

This chapter is a reprint of the paper "Phytoplankton niche generation by interspecific stoichiometric variation" published in Global Biogeochemical Cycles, with permission by the American Geophysical Union.
Citation: Göthlich, L., and A. Oschlies (2012), Phytoplankton niche generation by interspecific stoichiometric variation, Global Biogeochemical Cycles, 26, GB2010, doi:10.1029/2011GB004042.

Abstract

For marine biogeochemical models used in simulations of climate change scenarios, the ability to account for adaptability of marine ecosystems to environmental change becomes a concern. The potential for adaptation is expected to be larger for a diverse ecosystem compared to a monoculture of a single type of (model) algae, such as typically included in biogeochemical models. Recent attempts to simulate phytoplankton diversity in global marine ecosystem models display remarkable qualitative agreement with observed patterns of species distributions. However, modelled species diversity tends to be systematically lower than observed and, in many regions, is smaller than the number of potentially limiting nutrients. According to resource competition theory, the maximum number of coexisting species at equilibrium equals the number of limiting resources. By simulating phytoplankton communities in a chemostat model and in a global circulation model, we show here that a systematic underestimate of phytoplankton diversity may result from the standard modelling assumption of identical stoichiometry for the different phytoplankton types. Implementing stoichiometric variation among the different marine algae types in the models allows species to generate different resource supply niches via their own ecological impact. This is shown to increase the level of phytoplankton coexistence both in a chemostat model and in a global self-assembling ecosystem model.

3.1 Introduction

Owing to global warming, environmental conditions controlling upper ocean biological production are expected to change significantly during this century: Rising surface temperatures and enhanced fresh-water input are expected to result in shallower mixed layers, leading to reduced upper-ocean nutrient supply (Sarmiento et al., 1998). In the oligotrophic areas of the tropical and subtropical ocean, this may cause a decline in phytoplankton abundance and primary production (Behrenfeld et al., 2006; Boyce et al., 2010). Additionally, oligotrophic areas are expanding, which further decreases global ocean productivity (Gregg et al., 2005; Polovina et al., 2008).

Marine plankton ecosystems are thus experiencing considerable environmental changes. Responses include changes in species physiology, species distribution and community composition (Hays et al., 2005; Richardson and Schoeman, 2004; Hoegh-Guldberg and Bruno, 2010). Still, the adaptation potential of marine ecosystems to environmental changes is poorly known, making estimates about their future evolution problematic. This even holds for phytoplankton at the base of the marine food chain and being an important agent in the cycling of nutrients and carbon.

Modelling adaptive responses of phytoplankton to climate change requires a sufficiently diverse model community to allow for an adequate representation of the potential for adaptation (McCann, 2000). Approaches to model phytoplankton diversity have been developed recently (Bruggeman and Kooijman, 2007; Follows et al., 2007; Shoresh et al., 2008; Dutkiewicz et al., 2009), but frequently, a single numerical phytoplankton species tends to outcompete most or all of the others (Gregg et al., 2003; Follows et al., 2007; Dutkiewicz et al., 2009; Sinha et al., 2010; Barton et al., 2010). This situation matches the well-known paradox of the plankton as formulated by Hutchinson (1961):

> "The problem that is presented by the phytoplankton is essentially how it is possible for a number of species to coexist in a relatively isotropic or unstructured environment all competing for the same sorts of materials. ... According to the principle of competitive exclusion (Hardin, 1960) ... we should expect that one species alone would outcompete all the others so that in a final equilibrium situation the assemblage would reduce to a population of a single species."

Proposed solutions to the paradox, i.e. explanations for the observed phytoplankton diversity include environmental spatial and/or temporal heterogeneity, internally generated non-equilibrium dynamics as well as biological factors promoting diversity (Roy and Chattopadhyay, 2007). Among the latter are different life-history patterns, differential resource use and keystone predation (Armstrong and McGehee, 1980). The present study focusses exclusively on differential resource use as presented by Tilman (Tilman, 1980) as a means of maintaining phytoplankton coexistence in biogeochemical models.

3.1.1 Theoretical Background

The reason for the extinctions in recent phytoplankton models (Bruggeman and Kooijman, 2007; Follows et al., 2007; Shoresh et al., 2008; Dutkiewicz et al., 2009) can be deduced using the R^* concept (Dutkiewicz et al., 2009), which is part of Tilman's resource competition theory (Tilman, 1980): In steady state, a monoculture of any species reduces the concentration of its limiting resource to the lowest concentration allowing for its survival (R^*), hence growth rate equals losses. In a multi-species assemblage, the species requiring the lowest resource concentration will set the equilibrium resource concentration to its resource requirement R^*, which is too low for any other species to survive. Yet in practice, there is no steady state and species must avoid exclusion only for the timescale of the system under consideration, which is usually several orders of magnitude longer than the lifetime of a phytoplankton cell. Species with very similar R^*s may coexist for long enough to survive in the ocean (Dutkiewicz et al., 2009).

For coexistence of several species in a steady-state system with two or more resources, each species must be limited by a different resource, for which is has a higher requirement than all of its competitors (Petersen, 1975; Tilman, 1980). For n resources, this implies that at most n species can coexist. Yet in many models with multiple potentially limiting resources, the number of surviving species rarely reaches the number of limiting resources (Follows et al., 2007; Shoresh et al., 2008; Dutkiewicz et al., 2009).

3.1.2 Scope of This Study

To explain these earlier findings and to explore the potential of a simple and plausible model alteration in enhancing coexistence, we simulated phytoplankton communities in a simple chemostat (Petersen, 1975; Huisman and Weissing, 1999; Shoresh et al., 2008)

and in a global ocean model with a self-assembling phytoplankton community (Follows et al., 2007; Dutkiewicz et al., 2009). In both models, each resource and phytoplankton species are modelled individually. Each species i is characterised by its half-saturation constants $K_{j,i}$ for the uptake of each nutrient j (for details see section 3.2.1), the stoichiometric ratio (i.e. the relative resource content) $C_{j,i}$ of each resource j with respect to carbon (chemostat model) or phosphorus (global model), and its maximum growth rate r_i. The impact of these parameters on coexistence are evaluated by numerical simulations of randomly assembled plankton communities. Particular attention is paid to the effects of varying the species' stoichiometric coefficients $C_{j,i}$, since in global plankton models those are commonly parameterised according to the Redfield Ratio (Redfield, 1934; Gregg et al., 2003; Dutkiewicz et al., 2009), so that all species have the same stoichiometry ($C_{j,i} = C_j$ for every species i). We compared modelled diversity in runs with identical stoichiometry (molar N:C=0.15, P:C=9.4×10^{-3}, Si:C=0.15, Fe:C=1.175×10^{-5} (Redfield, 1934; Follows et al., 2007), Si only in chemostat model) to modelled diversity in simulations with stoichiometry drawn randomly from a $\pm25\%$ range around those values.

3.2 Model Description

3.2.1 Chemostat Model

The standard model of resource competition in a chemostat (Petersen, 1975; Tilman, 1980) uses a Monod nutrient uptake function for the phytoplankton. The Monod equation originally describes growth as a saturating function of a single external resource concentration: Growth of species i is assumed proportional to $r_i R_j/(K_{ji} + R_j)$ for resources R_j and half-saturation constants $K_{j,i}$ and a maximum possible growth rate r_i. In this formulation, $K_{j,i}$ is the external resource concentration R_j at which half of the maximum growth rate r_i is achieved, i.e. the half-saturation constant. Since in the present study, several external resources are modeled, of which only one determines the growth rate at a given point in time, the Monod equation is used to determine the potential uptake for each resource separately, while only the most limiting resource determines a species' actual growth rate (Liebig's law of the minimum).

Half-saturation constants for each resource were drawn randomly from the ranges suggested by Follows et al. (2007). The stoichiometry of the individual species is fixed, and all species take up all resources. Thus, every species influences every resource and vice

versa. Maximum growth rates were identical for all phytoplankton species in all experiments as was mortality, solely determined by the dilution rate. The model equations are as follows (for definitions of variables and parameters see table 3.1, for parameter values and ranges see table 3.2):

$$\frac{dP_i}{dt} = P_i(\mu_i(R_1, ..., R_k) - D) \qquad i = 1, ..., n \quad (3.1)$$

$$\frac{dR_j}{dt} = D(S_j - R_j) - \sum_{i=1}^{n} C_{ji}\mu_i(R_i, ..., R_k)P_i \qquad j = 1, ..., k \quad (3.2)$$

$$\mu_i(R_1, ..., R_k) = min\left(\frac{r_i R_1}{K_{1i}+R_1}, ..., \frac{r_i R_k}{K_{ki}+R_k}\right) \quad (3.3)$$

The chemostat model was initialised with 8 species and 4 resources, namely nitrate, phosphate, silicate, and iron, and run for 20 years. Concentrations of nutrient supply were 16 μmol NO_3/l, 16 μmol SiO_2/l, 1 μmol PO_4/l and 0.0125 μmol Fe/l. Each different model configuration was run 50 times with different parameter sets owing to the random assignments involved. Phytoplankton was initialised with a concentration of 1 μmol C/l. Any species reaching a concentration of less than $10^{-8}\mu$mol C/l was considered extinct and was removed from the system. This ensured numerical stability and prevented the unrealistic re-appearance of a practically extinct species in unstable systems. For the number of surviving species, only species with a concentration of $\geq 10^{-3}\mu$mol C/l were taken into account.

Table 3.1: Parameters and variables

Symbol	Definition	Unit
P_i	abundance of species i	$\mu mol\ C/l$ (chemostat model) $\mu mol\ P/l$ (global model)
R_j	concentration of resource j	$\mu mol/l$
μ_i	growth rate of species i	$1/d$
$C_{j,i}$	stoichiometric coefficient of resource j for species i	$mol/mol\ C$ (chemostat model) $mol/mol\ P$ (global model)
$K_{j,i}$	half-saturation constant of species i for uptake of resource j	$\mu mol/l$
r_i	maximum growth rate of species i	$1/d$
S_j	concentration of supply of resource j	$\mu mol/l$
D	dilution rate	$1/d$
k	number of resources	-
n	number of species	-

Table 3.2: Parameter values in chemostat model

Parameter	Definition	Min	Max	Unit
K_{NO_3}	half-saturation constant NO_3	0.24	0.56	$\mu mol/l$
K_{PO_4}	half-saturation constant PO_4	0.0135	0.035	$\mu mol/l$
K_{SiO_2}	half-saturation constant SiO_2	0.24	0.56	$\mu mol/l$
K_{Fe}	half-saturation constant Fe	1.7×10^{-5}	4.4×10^{-5}	$\mu mol/l$
C_N	stoichiometric coefficient N (cellular N:C)	0.135	0.165	$mol\ N/mol\ C$
C_P	stoichiometric coefficient P (cellular P:C)	8.46×10^{-3}	10.34×10^{-3}	$mol\ P/mol\ C$
C_{Si}	stoichiometric coefficient Si (cellular Si:C)	0.135	0.165	$mol\ Si/mol\ C$
C_{Fe}	stoichiometric coefficient Fe (cellular Fe:C)	1.058×10^{-5}	1.293×10^{-5}	$mol\ Fe/mol\ C$
C_N^*	Redfield N:C	0.15	–	$mol\ N/mol\ C$
C_P^*	Redfield P:C	9.4×10^{-3}	–	$mol\ P/mol\ C$
C_{Si}^*	Redfield Si:C	0.15	–	$mol\ Si/mol\ C$
C_{Fe}^*	Redfield Fe:C	1.175×10^{-5}	–	$mol\ Fe/mol\ C$
r_i	max. growth rate	2.0	–	$1/d$
D	dilution rate	0.25	–	$1/d$
S_{NO_3}	NO_3 supply	16	–	$\mu mol/l$
S_{PO_4}	PO_4 supply	1	–	$\mu mol/l$
S_{SiO_2}	SiO_2 supply	16	–	$\mu mol/l$
S_{Fe}	Fe supply	0.0125	–	$\mu mol/l$

3.2.2 Global Model

The global marine ecosystem model is a modified version of the self-assembling marine ecosystem model by Follows et al. (2007) comprising 78 phytoplankton and 2 zooplankton types. It explicitly resolves ocean circulation and mixing on a $1 \times 1^\circ$ grid with 23 depth levels. This model has previously been examined with regard to resource competition theory (Dutkiewicz et al., 2009; Barton et al., 2010) and this approach is extended in this study by including the effect of species-dependent phytoplankton stoichiometry.

The global model explicitly simulates the nutrients phosphorus, nitrate, nitrite, ammonia, silicate and iron, with phosphorus being used as the currency nutrient. It uses one prognostic equation for each of the 78 phytoplankton types and the 2 zooplankton types. Phytoplankton growth depends on light, nutrients, and temperature, while phytoplankton mortality is due to grazing, sinking, and a non-specific linear mortality.

The original Follows et al. (2007) model randomly assigns parameter values (from predefined ranges) for temperature, light, and nutrient dependence to 78 different phytoplankton types. For this study, the version of Dutkiewicz et al. (Dutkiewicz et al.,

2009) is used, but all randomness with regard to light and temperature dependence is removed. Of the originally 4 different functional phytoplankton types only the small functional type is used, albeit with a slightly increased maximum growth rate and the ability to use all forms of nitrogen (nitrate, nitrite and ammonia). Since all 78 phytoplankton types are of the same type and their nutrient uptake parameters are drawn from the same range, all competitive exclusion is due to differences in nutrient uptake capacity and not due to other interspecific variations. For the detailed parameter values see table 3.3. Diatoms are not simulated in this study, hence silicate parameters are omitted.

Since for equilibrium coexistence it is crucial that each species is a poor competitor for at least one of the resources, a simple trade-off between different Ks for each species was introduced: K_{PO_4} is drawn randomly from the range defined in table 3.3:

$$K_{PO_4} = K_{PO_4}^{min} + rand_1 * (K_{PO_4}^{max} - K_{PO_4}^{min}) \tag{3.4}$$

where $rand$ is a random number distributed uniformly between 0 and 1. The difference between K_{PO_4} and $K_{PO_4}^{min}$ is then used to generate K_{NO_3} in such a way that a species with a low K_{PO_4} has a high K_{NO_3} and vice versa:

$$K_{NO_3} = K_{NO_3}^{max} - \frac{K_{PO_4} - K_{PO_4}^{min}}{K_{PO_4}^{max} - K_{PO_4}^{min}} * (K_{NO_3}^{max} - K_{NO_3}^{min}) \tag{3.5}$$

A new random number between 0 and 1 is used to allow for 10% variability:

$$K_{NO_3} = K_{NO_3} \pm 0.1 * rand_2 * K_{NO_3} \tag{3.6}$$

K_{Fe} is traded off against K_{NO_3} in the same way:

$$K_{Fe} = K_{Fe}^{max} - \frac{K_{NO_3} - K_{NO_3}^{min}}{K_{NO_3}^{max} - K_{NO_3}^{min}} * (K_{Fe}^{max} - K_{Fe}^{min}) \tag{3.7}$$

$$K_{Fe} = K_{Fe} \pm 0.1 * rand_3 * K_{Fe} \tag{3.8}$$

This leads to K_{Fe} and K_{PO_4} being positively correlated, but iron and phosphate limitation do not spatially coincide in this model (see Figure 3.1). So this lack of a trade-off was accepted for simplicity.

K_{NO_2} and K_{NH_4} are assigned relative to K_{NO_3}:

$$K_{NO_3} = K_{NO_2} = 2 * K_{NH_4} \tag{3.9}$$

Stoichiometry in the runs with species-specific stoichiometry is proportional to the ratios of the Ks, i.e. $C_{x:P} = K_x/K_{PO_4}$. The ratio of P to carbon is assigned so that a species with a high K_{PO_4} has a high $C_{P:C}$, i.e. a species likely to be limited by PO_4 also consumes a lot of PO_4. This facilitates the occurrence of stable equilibrium conditions (for details see section 3.3.2). In the runs with Redfield stoichiometry, the Ks are the same as in those with species-specific stoichiometry, whereas the Cs are the same as in the original model.

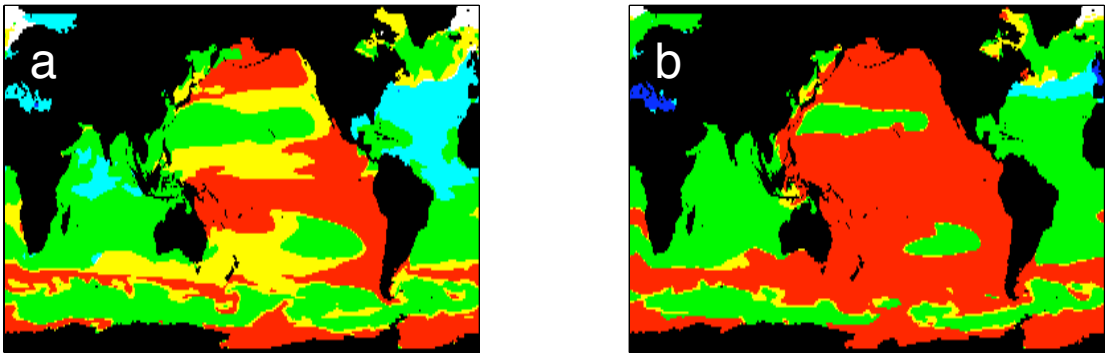

Figure 3.1: Limiting nutrient of all species in year 10 of the integration, upper 5 m; a: species-specific stoichiometry, b: Redfield stoichiometry; green: N limitation only; red: Fe limitation only; blue: P limitation only; mixtures indicate limitation of different algae by different nutrients, regardless of the respective number of species each; cyan: N and P limitation; yellow: N and Fe limitation; magenta: P and Fe limitation.

3.3 Chemostat Model Results

3.3.1 Redfield Stoichiometry

In a first set of chemostat experiments all species are assigned the same stoichiometry. The first configuration, $C_{\mathrm{Redf}}K_{\mathrm{rand}}$, uses Redfield stoichiometry and randomly chosen half-saturation constants $K_{j,i}$ for the different resources j and species i. Altogether, 50 simulations are performed, each starting with 8 random species and 4 resources, hence the equilibrium number of species cannot exceed 4. After 20 years, the number of surviving phytoplankton species rarely exceeds one and never exceeds two (Figure 3.2a).

Table 3.3: Parameter values in global model

Parameter	Definition	Min	Max	Unit
K_{PO_4}	half-saturation constant PO_4	0.015	0.035	μM
K_{NO_3}	half-saturation constant NO_3	0.18	0.70	μM
K_{NO_2}	half-saturation constant NO_2	0.18	0.70	μM
K_{NH_4}	half-saturation constant NH_4	0.09	0.35	μM
K_{Fe}	half-saturation constant Fe	1.125×10^{-5}	4.375×10^{-5}	μM
$C_{N:P}$	stoichiometric coefficient N (cellular N:P)	12	20	$mol\ N/mol\ P$
$C_{C:P}$	stoichiometric coefficient C (cellular C:P)	90	150	$mol\ C/mol\ P$
$C_{Fe:P}$	stoichiometric coefficient Fe (cellular Fe:P)	0.75×10^{-3}	1.25×10^{-3}	$mol\ Fe/mol\ P$
$C^*_{N:P}$	Redfield N:P	16	–	$mol\ N/mol\ C$
$C^*_{C:P}$	Redfield C:P	120	–	$mol\ C/mol\ P$
$C^*_{Fe:P}$	Redfield Fe:P	1.0×10^{-3}	–	$mol\ Fe/mol\ P$
r_i	max. growth rate	2.2	–	$1/d$
m_i	mortality	0.1	–	$1/d$

20 years is a typical advective timescale for an oligotrophic gyre, an oceanic system to which a chemostat model is closer than to more dynamic systems with shorter timescales.

In the second set of experiments, it was considered that careful ranking of the different equilibrium resource concentrations $R^*_{i,j}$ for each resource j can enhance coexistence (Huisman and Weissing, 2001): Each species has to be the worst competitor for one resource, i.e. for every resource j one species i has the maximum R^*_j. This ensures that each species is limited by a different resource, namely the one for which it has the highest R^*. Since in this chemostat model, maximum growth rates r_i and mortality (i.e. dilution) rates D are identical for all species, differences in R^* are solely determined by the half-saturation constants $K_{j,i}$ ($R^*_{i,j} = K_{j,i}D/(r - D)$). This configuration is referred to as $C_{\mathrm{Redf}}K_{\mathrm{rank}}$, and uses half-saturation constants $K_{j,i}$ so that two species are limited by resource one, two species by resource two etc., of which at most one species is expected to survive. However, also in configuration $C_{\mathrm{Redf}}K_{\mathrm{rank}}$ the number of coexisting species rarely exceeds one and never exceeds two (Figure 3.2a).

The chemostat simulations using the same (Redfield) stoichiometry for all species with random half-saturation constants for nutrient uptake do not allow for steady-state phytoplankton coexistence, in agreement with earlier theoretical studies (Tilman, 1980; Huisman and Weissing, 2001). Since in all simulations the maximum growth rate r_i is the same for all species, one might argue whether more species might coexist for species-

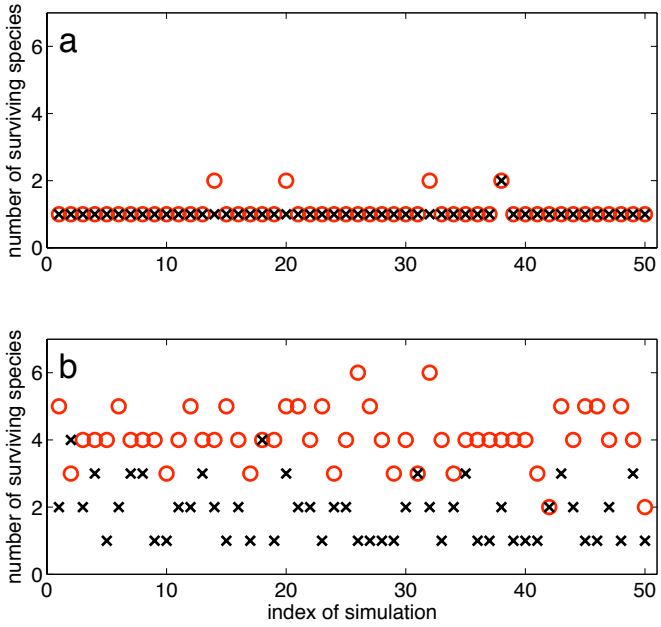

Figure 3.2: Number of surviving species at the end of 50 simulations over 20 years each; a: configurations $C_{\mathrm{Redf}}K_{\mathrm{rand}}$(black crosses) and $C_{\mathrm{Redf}}K_{\mathrm{rank}}$(red circles) and b: configurations $C_{\mathrm{eq}}K_{\mathrm{rand}}$(black crosses) and $C_{\mathrm{eq}}K_{\mathrm{rank}}$(red circles). Model configurations are described in table 3.4.

specific values of r_i. Following Shoresh et al. (2008) it can, however, be shown that stable coexistence is impossible when all species obey the same stoichiometry, irrespective of their maximum growth rates (see appendix).

3.3.2 Interspecies stoichiometric variations

Another series of simulations was run using different stoichiometries among the different species with $C_{j,i}$ assigned to match the conditions for coexistence (Huisman and Weissing, 2001): Each species consumes most of the resource by which it is limited; $K_{j,i}$ are assigned randomly in configuration $C_{\mathrm{eq}}K_{\mathrm{rand}}$, and for each resource j the species i with highest $K_{j,i}$ gets the highest value of $C_{j,i}$ among all species. In configuration $C_{\mathrm{eq}}K_{\mathrm{rank}}$, the $K_{j,i}$ and $C_{j,i}$ are assigned according to equilibrium conditions so that each species is limited by the resource of which it consumes most. For details on the parameterisation

see tables 3.2 and 3.4.

For the same random choices of $K_{j,i}$ as in the two respective Redfield experiments, the chance for coexistence increases significantly in the simulations with species-specific stoichiometries chosen such that each species consumes most of the resource for which it has the highest requirement (Figure 3.2): Among all simulation experiments performed, the by far highest number of coexisting phytoplankton species (4.08 ± 0.85) is reached in experiment $C_{\text{eq}}K_{\text{rank}}$, for which the $K_{j,i}$ and the $C_{j,i}$ are chosen so that both the conditions for the existence of a 4-species-equilibrium ($K_{j,i}$) and the conditions for said equilibrium to be stable ($C_{j,i}$) are met. Whenever species numbers exceed 4 (number of resources), competitive exclusion is not yet complete. Incomplete exclusion also occurred in the other configurations, which reach average numbers of coexisting species of 1.84 ± 0.87 in experiment $C_{\text{eq}}K_{\text{rand}}$, 1.08 ± 0.27 in $C_{\text{Redf}}K_{\text{rank}}$ and 1.02 ± 0.14 in $C_{\text{Redf}}K_{\text{rand}}$.

3.4 Global Model Results

The results of the global model mirror those of the chemostat model: phytoplankton diversity is, on average, higher in the run with species-specific stoichiometry compared to the run employing Redfield stoichiometry for all species (see Figure 3.3). Diversity is distinctly increased in the North Atlantic, the North Pacific and the Indian Ocean, whereas in the South Pacific and the Southern Ocean the difference is less pronounced. The cause and implication of these results are discussed in section 3.5.2.

3.5 Discussion

3.5.1 Chemostat Model

In the chemostat experiments, only species-specific stoichiometric ratios chosen in such a way that each species consumes most of the resource for which it has the highest requirement among the coexisting species (highest half-saturation constant $K_{j,i}$ for a given resource j) allows for coexistence with each species being limited by a different resource. This conclusion is consistent with those of earlier studies (Petersen, 1975; Tilman, 1980). This stability criterion was extended analytically to a hypothetical three-resource sys-

Table 3.4: Parameter assignment for chemostat simulations

configuration	$K_{j,i}$	$C_{j,i}$	details $K_{j,i}$	details $C_{j,i}$
$C_{\mathrm{Redf}}K_{\mathrm{rand}}$	random	Redfield	randomly from ranges defined in table 3.2	$C_{j,i} = C^*_j$, see table 3.2
$C_{\mathrm{Redf}}K_{\mathrm{rank}}$	ranked	Redfield	as in experiment $C_{\mathrm{Redf}}K_{\mathrm{rand}}$, with each K_{ii} increased (by a random amount of max. 10%) above the maximum of the predefined range, in order to obtain a rank order so that species 1 is the worst competitor for resource 1, species 2 is the worst competitor for resource 2, etc.	$C_{j,i} = C^*_j$, see table 3.2
$C_{\mathrm{eq}}K_{\mathrm{rand}}$	random	equilibrium[b]	randomly from ranges defined in table 3.2	$C_{j,i}$ drawn randomly from the stoichiometric ranges of table 3.2. The $C_{j,i}$ for the species with highest $K_{j,i}$ for each resource j gets assigned a value 10% larger than the upper limit of this range.
$C_{\mathrm{eq}}K_{\mathrm{rank}}$	ranked	equilibrium[b]	as in experiment $C_{\mathrm{Redf}}K_{\mathrm{rand}}$, with each K_{ii} increased (by a random amount of max. 10%) above the maximum of the predefined range, in order to obtain a rank order so that species 1 is the worst competitor for resource 1, species 2 is the worst competitor for resource 2, etc.	$C_{j,i}$ drawn randomly from the stoichiometric ranges of table 3.2. The $C_{j,i}$ for the species with highest $K_{j,i}$ for each resource j gets assigned a value 10% larger than the upper limit of this range.

[b] conditions for stability of equilibrium according to Huisman and Weissing (2001).

tem by Huisman and Weissing (Huisman and Weissing, 2001). In the present study, it has been extended further to a four-resource system representing nitrate, phosphate, silicate, and iron, generally thought to be the most limiting nutrients in the global ocean (Falkowski et al., 1998). Parameters were chosen to resemble those of actual oceanic phytoplankton, thereby linking resource competition theory and global biogeochemical modelling applications.

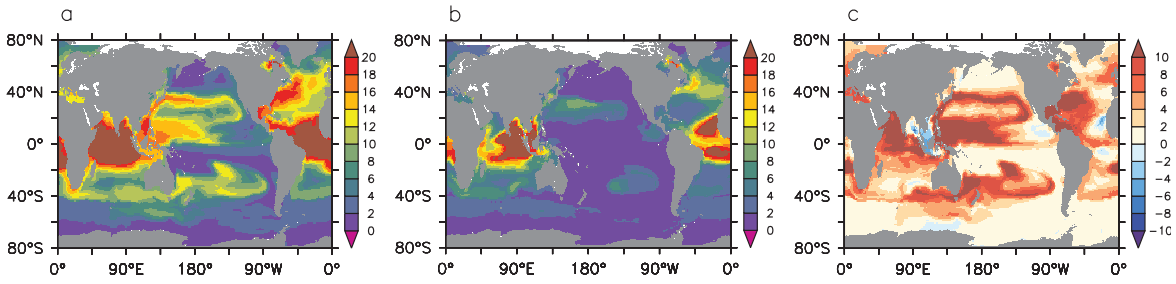

Figure 3.3: Number of surviving species in the upper 55 m of the global model after 10 years; a: 25% variability in stoichiometry, b: Redfield stoichiometry, c: difference.

3.5.2 Global Model

Both conditions for stable coexistence can also be attained in the global model simulations. Since in the original configuration (Dutkiewicz et al., 2009) the ratios of the different $K_{j,i}$ were identical for all species, all species in one place were almost always limited by the same resource. In the current study, the ratios of the different $K_{j,i}$ were allowed to vary between species, hence different species can be limited by different resources in one place.

In the Atlantic and Pacific, and to a lesser extent in the Indian and Southern Ocean, large areas show limitation by two nutrients in the species-specific-stoichiometry run (see Figure 3.1a, $75.36 * 10^6$ km^2 N and P limitation, $38.56 * 10^6$ km^2 N and Fe limitation). With Redfield stoichiometry applied, limitation of different algae by different nutrients is restricted to considerably smaller areas (see Figure 3.1b, $14.49 * 10^6$ km^2 N and P limitation, $5.55 * 10^6$ km^2 N and Fe limitation). Since stoichiometry determines nutrient uptake ratios in this model, this shows that nutrient uptake ratios can have considerable influence on nutrient concentrations in addition to their impact on diversity.

3.5.3 Niche Theory

Nutrient uptake ratios ($C_{j,i}$) are part of a species' ecological "impact niche", which is the impact an organism has on its environment by consuming resources (Leibold, 1995),

representing one of the two concepts of an ecological niche. The complementary niche concept is the "requirement niche", encompassing the impact of the environment on an organism. While the requirement niche, represented by $K_{j,i}$, is often paid attention in biogeochemical models including the one used in this study (Dutkiewicz et al., 2009; Barton et al., 2010), the impact niche is mostly ignored through the widespread implementation of constant (generally Redfield) stoichiometry, which essentially creates one identical impact niche for all species. Yet, in reality species do have different impacts on their environment and thereby influence the requirement niches of other species as well as their own. This connection is mirrored in the global model results presented in this study: Different nutrient uptake ratios (impact niches) lead to different species being limited by different resources (requirement niches). Identical nutrient uptake ratios impede that effect. In addition, the imposed positive correlation between the $C_{j,i}$ and the $K_{j,i}$ implies that through their impact niches, each species has a stronger influence on its own requirement niche than on that of other species. By taking up most of the nutrient it requires most, it limits its own growth more than it limits others, i.e. intraspecific competition is greater than interspecific competition, a mechanism that is known to promote diversity (Chesson, 2000; Tilman, 1980).

3.5.4 Parameter Choices

This positive correlation between the $C_{j,i}$ and the $K_{j,i}$ (or R^*) imposed in the model is supported by data for some of the nutrients used in this study: Different algae show strong positive correlation between C_{Si} and R^*_{Si} (Huisman and Weissing, 2001) and there is also evidence for a positive correlation between the minimum nitrogen content $C_{N_{min}}$ and half-saturation constants K_{NO_3} and K_{NH_4} (Litchman et al., 2007; Sunda and Hardison, 2010), respectively. Low C_{Fe} is found in small oceanic phytoplankton species with a high surface-to-volume ratio enabling fast nutrient uptake (low K_{Fe}). Coastal phytoplankton have higher values for both parameters (Sunda and Huntsman, 1995).

Besides the link between $C_{j,i}$s and $K_{j,i}$s, stable coexistence also assumes trade-offs between the $K_{j,i}$ for each species i. Data on R^* (Huisman and Weissing, 2001) show trade-offs for phosphate vs. silicate and nitrate vs. silicate in diatoms. For other resources, similar trade-offs are not known, but are considered plausible as a result of physiological limits on nutrient acquisition (Litchman and Klausmeier, 2008).

A next step towards simulating resource use and uptake by phytoplankton more realistically would be to explicitly simulate the changes in stoichiometry in response to ambient concentrations and phytoplankton growth. Available models with different levels of sophistication include Droop's cell quota model (Droop, 1973) as well as Pahlow's optimal growth model using explicit dynamics for various phytoplankton properties (Pahlow, 2005; Pahlow and Oschlies, 2009). However, such models are computationally more expensive and differ in more than one aspect with respect to the standard constant-stoichiometry model version. The current study attempts to apply a minimum variation to the standard model and thereby conclusively attribute all changes in model dynamics to the only change of allowing small variations in the phytoplankton's stoichiometry.

3.6 Conclusion

While it is unclear whether the proposed mechanism of stoichiometrically generated impact niches is crucial in maintaining phytoplankton diversity in the ocean, there is sufficient data showing that the Redfield Ratio is only valid when averaging over many species. Individual species' stoichiometric coefficients differ from one another, and those of one species differ in time and space (Geider and La Roche, 2002; Anderson and Pondaven, 2003; Klausmeier et al., 2004). Combining the findings of this study with evidence from data supports the need for going beyond the Redfield Ratio as a common stoichiometry in models with multiple phytoplankton compartments. Instead, species' resource contents should vary across species, and, if coexistence in models is to be sustained to allow for conclusions about environmentally induced changes in community compositions, the conditions for stable coexistence should be considered.

Acknowledgments

The authors thank S. Dutkiewicz (MIT) for providing the global model code and F. Prowe (IFM-GEOMAR) for running the global model simulations. L.G. acknowledges funding by WGL-PAKT, project TiPI and the Deutsche Forschungsgemeinschaft (DFG) via SFB 754.

3.7 Appendix: Analysis of Redfield Case

In the following section, the stability of a multispecies equilibrium with the same stoichiometry assigned to all species is analysed in detail. Assuming the $R^*_{i,j}$, dependent on half-saturation constants, dilution and maximum uptake rate, are chosen in such a way that each species i is limited by a different resource j (species 1 by resource 1, species 2 by resource 2 and so on), Shoresh et al. (2008) derived the general conditions for a given equilibrium to be stable, based on the steady-state solution of equations 1 and 2.

$$\frac{dP_i}{dt} = P_i\left(\frac{r_i R_i}{K_{ii}+R_i} - D\right) = 0 \longleftrightarrow \mathbf{R}^* = \frac{D\mathbf{K}}{r-D} \quad (3.10)$$

$$\frac{dR_j}{dt} = D\left(S_j - R_j\right) - \sum_{i=1}^{n} C_{ji} P_i \frac{r_i R_i}{K_{ii}+R_i} = 0 \longleftrightarrow \mathbf{P}^* = \mathbf{C^{-1}}(\mathbf{S} - \frac{D\mathbf{K}}{r-D}) \quad (3.11)$$

and using the following vector notation:

$$\mathbf{P} = \begin{pmatrix} P_1 \\ \vdots \\ P_n \end{pmatrix},\ \mathbf{K} = \begin{pmatrix} K_{11} \\ \vdots \\ K_{nn} \end{pmatrix},\ \mathbf{S} = \left(\begin{array}{c} S_1 \\ \vdots \\ S_n \\ \hline S_{n+1} \\ \vdots \\ S_k \end{array}\right),\ \mathbf{R} = \left(\begin{array}{c} R_1 \\ \vdots \\ R_n \\ \hline R_{n+1} \\ \vdots \\ R_k \end{array}\right) = \begin{pmatrix} \bar{\mathbf{R}} \\ \hline \tilde{\mathbf{R}} \end{pmatrix},$$

$$\mathbf{C} = \left(\begin{array}{ccc} C_{11} & \dots & C_{1n} \\ \vdots & \ddots & \vdots \\ C_{n1} & \dots & C_{nn} \\ \hline C_{n+11} & \dots & C_{n+1n} \\ \vdots & \ddots & \vdots \\ C_{k1} & \dots & C_{kn} \end{array}\right) = \begin{pmatrix} \bar{\mathbf{C}} \\ \hline \tilde{\mathbf{C}} \end{pmatrix}.$$

Where $i = 1, ..., n$, with n being the number of species, $j = 1, ..., k$, with k being the number of resources and $n \leq k$, $C_{j,i}$ the stoichiometric coefficient of species i for resource j, $K_{i,i}$ the half-saturation constant of species i for its limiting resource, P^*_i the equilibrium concentration of species i, r_i the maximum growth rate of species i, D the dilution rate (=mortality).

Stability of the equilibrium solution (marked by an asterisk) can be investigated by adding a small perturbation δ and keeping only terms that are linear in δ:

$\mathbf{P} = \mathbf{P}^* + \delta\mathbf{P}$, $\bar{\mathbf{R}} = \bar{\mathbf{R}}^* + \delta\bar{\mathbf{R}}$ and $\tilde{\mathbf{R}} = \tilde{\mathbf{R}}^* + \delta\tilde{\mathbf{R}}$.

This leads to

$$\frac{d}{dt}\begin{pmatrix} \delta\mathbf{P} \\ \delta\bar{\mathbf{R}} \\ \delta\tilde{\mathbf{R}} \end{pmatrix} = \mathbf{J}\begin{pmatrix} \delta\mathbf{P} \\ \delta\bar{\mathbf{R}} \\ \delta\tilde{\mathbf{R}} \end{pmatrix} \tag{3.12}$$

with the Jacobian

$$\mathbf{J} = \begin{pmatrix} 0 & \mathbf{A} & 0 \\ -D\bar{\mathbf{C}} & -D\bar{\mathbf{I}} - \bar{\mathbf{F}} & 0 \\ -D\tilde{\mathbf{C}} & \tilde{\mathbf{F}} & -D\tilde{\mathbf{I}} \end{pmatrix},$$

with

$$\mathbf{A}_{n\times n} = \{A_{ij}\},\ A_{ij} = \frac{P_i^*(r_i - D)^2}{r_i K_{ii}}\,\delta_{ij},\ i,j = 1,...,n \tag{3.13}$$

$$\bar{\mathbf{F}}_{n\times n} = \{\bar{F_{ji}}\},\ \bar{F_{ji}} = C_{ji}A_{ii},\ i,j = 1,...,n \tag{3.14}$$

$$\tilde{\mathbf{F}}_{(k-n)\times n} = \{\tilde{F_{ji}}\},\ \tilde{F_{ji}} = C_{ji}A_{ii},\ j = n+1,...,k, i = 1,...,n \tag{3.15}$$

and $\bar{\mathbf{I}}_{n\times n}$ and $\tilde{\mathbf{I}}_{(k-n)\times(k-n)}$ being identity matrices.

For the equilibrium to be stable, all eigenvalues of $\mathbf{J}$ need to be negative. Shoresh et al. (2008) then derive that this is the case if and only if all the eigenvalues of the matrix $\bar{\mathbf{F}}$ with

$$\bar{F_{ji}} = \frac{(r_i - D)^2 C_{ji} P_i^*}{r_i K_{ii}^*} \tag{3.16}$$

are positive. Setting C_{ji} in such a way that all species are assigned the same stoichiometry (i.e. $C_{j1} = C_{j2}, ..., = C_{jn}$ etc.) leads to

$$\bar{F_{ji}} = \frac{(r_i - D)^2 C_j P_i^*}{r_i K_{ii}^*}. \tag{3.17}$$

Since r_i, K_{ii}^* and P_i^* differ only between species, while C_j differs only between resources, $\bar{F_{ji}}$ can be split into the resource-dependent part C_j and a species-dependent term B_i, so that

$$B_i = \frac{(r_i - D)^2 P_i^*}{r_i K_{ii}^*}. \tag{3.18}$$

Accordingly simplified, $\bar{\mathbf{F}}$ becomes

$$\bar{F}_{ji} = \begin{vmatrix} B_1C_1 & B_2C_1 & \dots & B_nC_1 \\ B_1C_2 & B_2C_2 & \dots & B_nC_2 \\ \vdots & \vdots & \ddots & \vdots \\ B_1C_n & B_2C_n & \dots & B_nC_n \end{vmatrix}.$$

The rows of $\bar{\mathbf{F}}$ differ only by a factor (C_j) and are therefore linearly dependent, hence all eigenvalues of $\bar{\mathbf{F}}$ except one are zero. Accordingly, the equilibrium point is not stable and all but one species will go extinct. Note that the instability of an equilibrium with coexisting species holds irrespective of whether or not the maximum growth rate r_i varies between species.

4 External disturbance emphasizes the benefit of stoichiometric variation in maintaining diversity in phytoplankton models

This chapter is also a manuscript in preparation by L. Göthlich and A. Oschlies.

4.1 Introduction

Numerical models used to simulate past, present and future ocean biogeochemistry commonly include a description of marine pelagic ecosystems. A key component of such descriptions is phytoplankton, which is responsible for roughly 50% of global photosynthesis and which, via photosynthetic CO_2 uptake, drives the marine biological carbon pump. Whenever environmental conditions change, as is the case with the current rise of CO_2 levels and temperatures, the ability of the pelagic ecosystem to (1) adapt to the changes and (2) continue its biogeochemical functioning becomes an issue. It is generally assumed that the ability of the planktonic system to adapt depends on how diverse the population is (McCann, 2000; Ptacnik et al., 2008).

In an attempt to make marine ecosystem models appear more realistic, some recent models have split the phytoplankton compartment into various functional types such as diatoms, non–diatoms, small phytoplankton and N_2–fixing organisms (Bruggeman and Kooijman, 2007; Shoresh et al., 2008; Dutkiewicz et al., 2009; Monteiro et al., 2010; Sinha et al., 2010). Resource competition theory states that in equilibrium, the number of coexisting species can equal the number of limiting resources (Tilman, 1980), yet in many biogeochemical models, one or few species frequently outcompete most or all of the others. This mimics the famous paradox of the plankton (Hutchinson, 1961), which essentially states that competitive exclusion should, in the rather uniform environment

of the pelagial, lead to dominance of a single species. Possible explanations for the seemingly paradoxical diversity in the real ocean include externally or internally generated variation, keystone predation, life histories and differential resource use.

In a recent modelling study, it was shown that implementing differential resource use *sensu* Tilman (1980) by means of stoichiometric differences between different marine algae types allows species to generate different resource supply niches via their own ecological impact, thereby increasing the level of phytoplankton diversity (Göthlich and Oschlies, 2012). This can explain the systematic underestimate of phytoplankton diversity in other modelling studies, which commonly employ identical stoichiometry for all species, fixed at the Redfield Ratio (Redfield, 1934; Gregg et al., 2003; Dutkiewicz et al., 2009; Barton et al., 2010). A necessary precondition for increased diversity through varied stoichiometry is that the species' resource requirements and resource contents (i.e. stoichiometry) follow Tilman's resource–ratio hypothesis (Tilman, 1980).

The above approach of allowing for interspecific stoichiometric variations was developed in a chemostat model and, although tested in a global model, was considered valid primarily for largely undisturbed ocean regions such as oligotrophic gyres. However, introducing species–specific stoichiometry increased global modelled phytoplankton not only in oligotrophic gyres, but also in more dynamic regions, indicating that the concept as a whole might also be valid under disturbance. To specifically address this point, simulated communities of ten different levels of diversity (1, 2, 3, 4, 8, 16, 24, 40, 80 and 120 species, respectively), each parameterised according to Tilman's resource–ratio hypothesis, were subjected to different modes of disturbance and run for 120 years. The remaining diversity, biomass and resource concentrations were analysed after 1, 5, 10, 20, 40, 80 and 120 years. Results were compared against those of the same experiments performed with phytoplankton communities whose internal stoichiometry was parameterised according to the Redfield Ratio. It was shown that interspecific stoichiometric variation indeed increases diversity under disturbance, showing the validity of the resource competition theory also for disturbed systems.

4.2 Methods

4.2.1 Model

The model used is a version of the standard model of resource competition (Petersen, 1975), parameterised as described in Göthlich and Oschlies (2012), modelling each resource and phytoplankton species individually. Each species i is characterised by its half–saturation constants $K_{i,j}$ for the Monod uptake of each nutrient j, the stoichiometric ratio $C_{i,j}$ of each resource j with respect to carbon, its species–specific mortality m_i in addition to the common dilution rate D, and its maximum growth rate r_i. Mortality does not result in nutrient recycling, as dead phytoplankton is assumed to sink out of the water column. Half–saturation constants for each resource were drawn randomly from the ranges suggested by Follows et al. (2007). Maximum growth rates were identical for all phytoplankton species in all experiments. Two basic model configurations were compared: (1) a Redfield configuration (hereafter named C_{Redf}) in which all stoichiometric ratios $C_{i,j}$ follow a constant Redfield ratio, i.e. $C_{i,j} = C_j^*$ with C_j^* given in table 4.2, and (2) a configuration that allows for a multispecies equilibrium (hereafter named C_{eq}), where stoichiometric ratios $C_{i,j}$ are chosen so that each species contains and therefore consumes most of the resource by which it is most likely limited (for details see table 4.3). The model equations are as follows (for definitions of variables and parameters see table 4.1, for parameter values and ranges see table 4.2):

Table 4.1: Parameters and variables

Symbol	Definition	Unit
P_i	abundance of species i	$\mu mol\ C/l$
R_j	concentration of resource j	$\mu mol/l$
μ_i	growth rate of species i	$1/d$
$C_{j,i}$	stoichiometric coefficient of resource j for species i	$mol/mol\ C$
$K_{j,i}$	half–saturation constant of species i for uptake of resource j	$\mu mol/l$
r_i	maximum growth rate of species i	$1/d$
S_j	concentration of supply of resource j	$\mu mol/l$
D	dilution rate	$1/d$
k	number of resources	-
n	number of species	-

$$\frac{dP_i}{dt} = P_i(\mu_i(R_1, ..., R_k) - D - m) \qquad i = 1, ..., n \quad (4.1)$$

$$\frac{dR_j}{dt} = D(S_j - R_j) - \sum_{i=1}^{n} C_{ji}\mu_i(R_i, ..., R_k)P_i \qquad j = 1, ..., k \quad (4.2)$$

$$\mu_i(R_1, ..., R_k) = min\left(\frac{r_i R_1}{K_{1i}+R_1}, ..., \frac{r_i R_k}{K_{ki}+R_k}\right) \quad (4.3)$$

Initially, a species pool comprising 120 species was generated according to the rules shown in table 4.3. Half–saturation constants are identical in the species pools of the Redfield experiment and of the variable–stoichiometry configuration. For simulations that require less than the total 120 species, 20 random subsets with the respective species number were generated and the model was run with each subset in all versions of the respective experiments defined below. For the monocultures with a single species only, each of the 120 species were used as single–species subset. Hence for the 1–species runs, there are 120 replicates each.

Parameters were chosen such that each species is potentially limited by one resource, such that for each of the four resources, there are 30 species that have a high $K_{i,j}$ for that particular resource. Yet the subsets of the initial 120 species set were drawn entirely randomly, hence in the subset runs the proportions of species limited by each resource are not controlled for.

4.3 Model Experiments

4.3.1 Chemostat

This baseline setup represents an undisturbed system that will reach equilibrium. It mimics a well–mixed chemostat culture with continuous and constant dilution. Nutrients are supplied with the inflow medium and the contents of the simulated culture vessel, including phytoplankton biomass, are removed at the same dilution rate D.

4.3.2 Disturbance modes

Two different disturbance modes were applied to the model: (1) semi–continuous culture, i.e. the system mimics a closed well–mixed culture vessel with dilution events taking place at fixed intervals. At dilution events, a certain fraction of the culture medium is removed

Table 4.2: Parameter values

parameter	definition	min	max	unit
K_{NO_3}	half–saturation constant NO_3	0.24	0.56	$\mu mol/l$
K_{PO_4}	half–saturation constant PO_4	0.0135	0.035	$\mu mol/l$
K_{SiO_2}	half–saturation constant SiO_2	0.24	0.56	$\mu mol/l$
K_{Fe}	half–saturation constant Fe	1.7×10^{-5}	4.4×10^{-5}	$\mu mol/l$
C_N	stoichiometric coefficient N (cellular N:C)	0.135	0.165	$mol\ N/mol\ C$
C_P	stoichiometric coefficient P (cellular P:C)	8.46×10^{-3}	10.34×10^{-3}	$mol\ P/mol\ C$
C_{Si}	stoichiometric coefficient Si (cellular Si:C)	0.135	0.165	$mol\ Si/mol\ C$
C_{Fe}	stoichiometric coefficient Fe (cellular Fe:C)	1.058×10^{-5}	1.293×10^{-5}	$mol\ Fe/mol\ C$
C_N^*	Redfield N:C	0.15	–	$mol\ N/mol\ C$
C_P^*	Redfield P:C	9.4×10^{-3}	–	$mol\ P/mol\ C$
C_{Si}^*	Redfield Si:C	0.15	–	$mol\ Si/mol\ C$
C_{Fe}^*	Redfield Fe:C	1.175×10^{-5}	–	$mol\ Fe/mol\ C$
r_i	max. growth rate	2.0	–	$1/d$
m_i	mortality	0.05	–	$1/d$
D	dilution rate	0.25	–	$1/d$
S_{NO_3}	NO_3 supply	16	–	$\mu mol/l$
S_{PO_4}	PO_4 supply	1	–	$\mu mol/l$
S_{SiO_2}	SiO_2 supply	16	–	$\mu mol/l$
S_{Fe}	Fe supply	0.0125	–	$\mu mol/l$

and immediately replaced with fresh medium. (2) Virus infections, a setup using random mortality events targeted at a single species to mimic species–specific virus attacks.

Semi–continuous culture

The semi–continuous culture disturbance mode was adapted from Gaedeke and Sommer (1986): disturbance is implemented as distinct dilution events, exchanging a specified fraction of the culture medium with inflow medium. Thereby, phytoplankton concentrations are reduced and nutrient concentrations are increased. Dilution intervals were set every 1, 2, 3, 5, 7, 10, 14, 21, and 28 days in the respective experiments, and the average long–time dilution rate was held constant at $0.25\,\mathrm{d}^{-1}$. Dilution intensity, or the fraction of volume exchanged at each dilution event, was calculated so that the same time–averaged instantaneous growth rate was required to overcome the loss caused by dilution (i.e. $0.25\,\mathrm{d}^{-1}$), irrespective of the respective dilution interval (see also Sommer, 1995): exchange fraction $V_{\mathrm{exch}}/V_0 = 1 - \mathrm{e}^{-d\,\tau}$, where d is dilution rate and τ is dilution interval. The resulting exchange fractions are shown in table 4.4 (see also appendix A). Among the setups used here, this semi–continuous culture setup is probably closest to

Table 4.3: Parameter assignment

$C_{j,i}$	details for assignment of $K_{j,i}$	details for assignment of $C_{j,i}$
Redfield	randomly from ranges defined in table 4.2, with each K_{ii} increased (by a random amount of max. 10%) above the maximum of the predefined range in order to obtain a rank order so that species 1 is the worst competitor for resource 1, species 2 is the worst competitor for resource 2, etc.	$C_{j,i} = C_j^*$, see table 4.2
equilibrium[b]	randomly from ranges defined in table 4.2, with each K_{ii} increased (by a random amount of max. 10%) above the maximum of the predefined range in order to obtain a rank order so that species 1 is the worst competitor for resource 1, species 2 is the worst competitor for resource 2, etc.	$C_{j,i}$ drawn randomly from the stoichiometric ranges of table 4.2. The $C_{j,i}$ for the species with highest $K_{j,i}$ for each resource j gets assigned a value 10% larger than the upper limit of this range.

[b] conditions for stability of equilibrium according to Tilman (1980).

conditions in the ocean, where deepening of the mixed layer, e.g. by mesoscale features in the ocean or storms in the atmosphere, can lead to nutrient pulses and at the same time dilute phytoplankton concentrations in the mixed layer.

Table 4.4: Fraction of medium exchanged at dilution events

τ (days)	V_{exch} (dim.less)
1	0.2212
2	0.3935
3	0.5276
5	0.7135
7	0.8262
10	0.9179
14	0.9698
21	0.9948
28	0.9991

Virus infection

To mimic possible disturbance events caused by virus infections, an intermittent species–specific mortality was introduced in addition to the existing mortality. At fixed intervals, one species gets "infected" by a virus, i.e. part of the species dies immediately. 75% of the organic matter of the respective species is instantaneously recycled back to inorganic nutrients, since virus mortality usually implies the bursting of the infected cell. The infection's target species was chosen randomly, the probability of infection being proportional to the species' relative abundance. Virus–induced mortality was also determined randomly, from the range $25 - 90\%$. Three infection intervals were implemented, 1 year, 5 years and 10 years.

4.4 Results

In the following, results are presented for representative subsets of the performed simulations for each setup: Semi–continuous culture with dilution every 1, 7 and 28 days; virus infection every 1 and 10 years. Output variables of interest include: (1) remaining species number as a measure of diversity and of whether species assemblies are stable over time; (2) Shannon index as a measure of diversity; (3) biomass (in carbon units) as a measure of productivity; and (4) concentrations of left–over resources as a measure for resource use efficiency. In this model system, carbon biomass can be used to assess productivity since nutrient input, mortality and dilution rate are identical between the C_{Redf} and C_{eq} configurations and for all initial diversity levels within the same disturbance mode. Therefore, differences in biomass between basic model configurations or between different diversity levels in the same disturbance mode are solely due to differences in productivity. This argument correspondingly applies to using resource concentration as a measure of resource use efficiency.

4.4.1 Disturbance effects on diversity

The number of surviving species in each setup after 1, 5, 10, 20, 40, 80 and 120 years was used to assess the stability of the different multi–species model–phytoplankton assemblages. In the steady–state chemostat system, at maximum 4 species can coexist on 4 resources, whereas away from equilibrium, diversity may be significantly higher (Hutchinson, 1961). Figure 4.1 shows the average number of surviving species in the different

systems for the simulations employing 40 initial species. The average long–term number of survivors in the undisturbed chemostat is close to 4 (4.30±0.57) in simulations using phytoplankton stoichiometry according to Tilman's resource–ratio hypothesis (Tilman, 1980, hereafter called C_{eq}). This result is considered in accordance with resource competition theory that predicts a maximum of 4 coexisting species, as competitive exclusion is not yet complete in some runs due to very similar or even identical half–saturation constants. This phenomenon also occurs in other models and is used to explain phytoplankton diversity e.g. in oligotrophic ocean regions (Barton et al., 2010). In the runs with Redfield stoichiometry (hereafter called C_{Redf}), a stable multi–species equilibrium does not exist (average long–term number of survivors: 1.05±0.22, see also Göthlich and Oschlies, 2012).

The overall pattern of higher long–term diversity in the C_{eq} simulations compared to C_{Redf} is preserved under all disturbance modes. In semi–continuous culture, species number in C_{eq} declines toward the equilibrium value reached in the chemostat simulations as well, albeit after a much longer period of competitive coexistence (long–term average species numbers after 120 simulated years are 5.00±0.65, 7.85±1.53, 10.95±1.43 for semi–continuous dilution every 1, 7 and 28 days, respectively). Also, the longer the disturbance interval, which is coupled to a higher intensity of the single dilution event, the longer it takes for species numbers to decline. Yet, the core set of species surviving is the same under all disturbance intervals of one replicate of species compositions.

The long–term theoretical equilibrium can easily be predicted from the phytoplankton parameters and is consistent with resource–competition theory: at maximum 4 species coexist at the intersection point of the resource requirements (R^*) of their respective limiting resources, provided they are limited by different resources. This equilibrium only exists if half–saturation constants are parameterised according to resource competition theory, i.e. so that each species is a poor competitor for one resource, by which, in consequence, it will be limited in equilibrium. For the given equilibrium to be stable, the stoichiometric coefficients need to mirror the half–saturation constants, i.e. each species needs to consume comparatively more of the resource by which it is limited (see table 4.3 and Tilman, 1980), which is not the case in the Redfield configuration. Thus, additional species surviving in the perturbation runs over the 120–year integration period considered here would go extinct if the model was run for an even longer time.

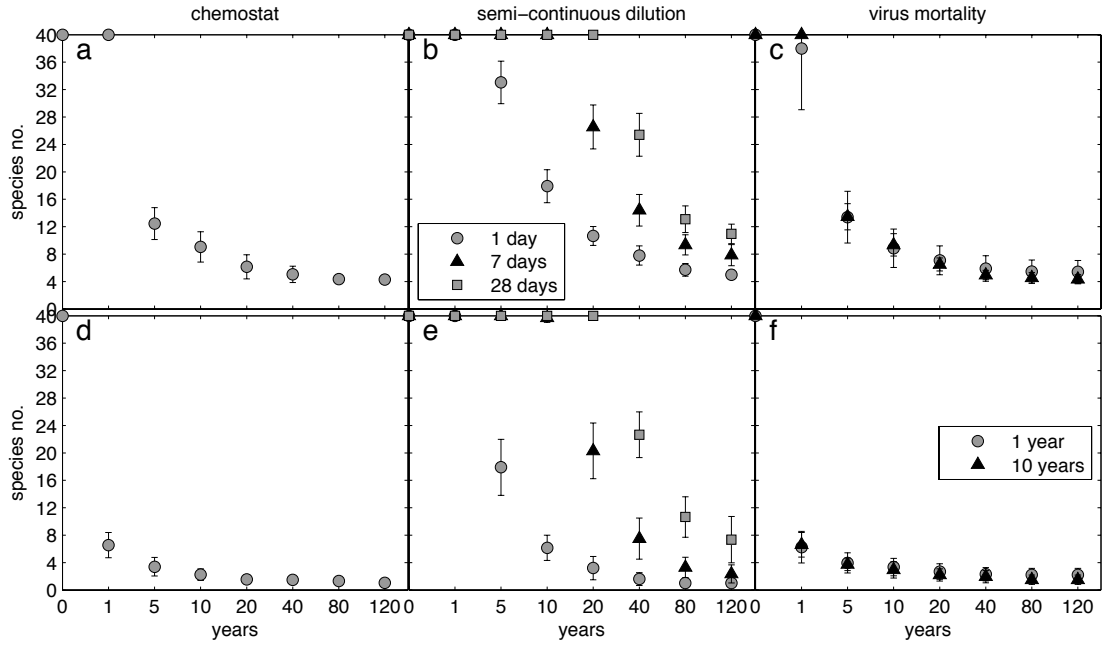

Figure 4.1: 40 phytoplankton species on 4 resources; number of surviving species after 1, 5, 10, 20, 40, 80 and 120 years, respectively, mean and standard deviation of replicate runs. Top row: simulations using equilibrium conditions on stoichiometry (C_{eq}), bottom row: Redfield stoichiometry (C_{Redf}). The different disturbance modes are: (a),(d) perfect chemostat (b),(e) semi–continuous culture with dilution every 1, 7, 28 days; (c),(f) chemostat with "virus infection" every 1 and 10 years.

Furthermore, this equilibrium can only be reached if the overall consumption vector, i.e. the vector connecting the equilibrium resource concentrations with the resource supply concentrations, lies within the range between the individual consumption vectors. For example, in a two–species equilibrium with species 1 limited by resource 1 and species 2 limited by resource 2, species 1 consumes more of resource 1 compared to species 2 and species 2 consumes more of resource 2. Hence, the resource supply point must be at an intermediate ratio of resource 1 to resource 2 for the equilibrium point to be reached.

This convergence toward the theoretical maximum number of coexisting species becomes even more evident if, instead of simply counting species number, the Shannon

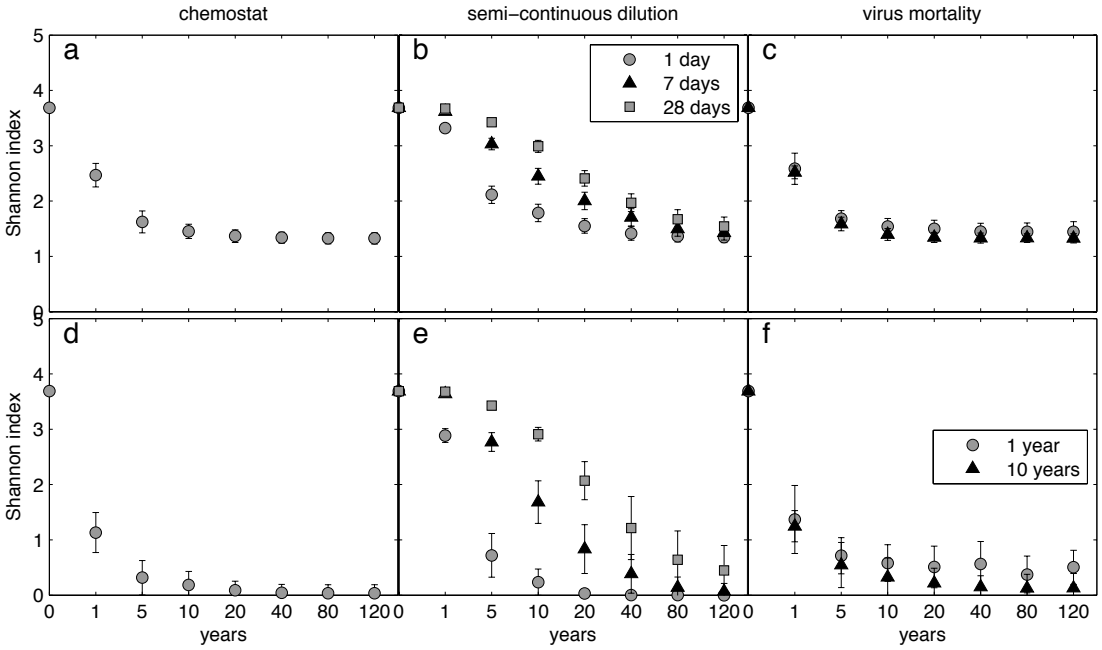

Figure 4.2: 40 phytoplankton species on 4 resources; Shannon diversity index after 1, 5, 10, 20, 40, 80 and 120 years, respectively, mean and standard deviation of replicate runs. Top row: simulations using equilibrium conditions on stoichiometry (C_{eq}), bottom row: Redfield stoichiometry (C_{Redf}). The different disturbance modes are: (a),(d) perfect chemostat; (b),(e) semi–continuous culture with dilution every 1, 7, 28 days; (c),(f) chemostat with "virus infection" every 1 and 10 years.

index is used to determine diversity. The Shannon diversity index H', calculated as $H' = \sum_i^n \left(\frac{P_i}{P_{\text{sum}}} ln \frac{P_i}{P_{\text{sum}}} \right)$, where n is number of species, P_i is biomass of species i and P_{sum} is total biomass, takes into account the evenness of the distribution of biomass among the competitors. The more similar the respective abundances, the higher the Shannon index, while dominance by a single species results in values close to zero. The index is likewise zero if only one species survives. Considering the Shannon index, the difference in long–term diversity between the chemostat and the semi–continuous dilution experiments becomes negligible (chemostat: 1.32±0.10, semi–continuous culture with 1, 7, 28–day dilution interval, respectively: 1.35±0.10, 1.43±0.13, 1.54±0.17). Hence, disturbance in this setting is only a means of delaying competitive exclusion, not of preventing it entirely. Yet in the real ocean, constant or repetitive periodically identical

conditions for timescales as long as 120 years do not occur, so disturbance events mimicked by semi–continuous culture most likely play a key role in sustaining phytoplankton diversity.

Similarly, under C_{Redf} parameterisation, the main effect of dilution events is also to delay competitive exclusion. Due to identical stoichiometry not allowing for stable coexistence, at equilibrium only one species survives, namely the one with the overall lowest R^* for its limiting resource. That is, the species with the overall highest growth rate on the given nutrient input eventually outcompetes all others. As in the C_{eq} simulations, the survivor can be predicted from the species' parameters. In the C_{Redf} runs, the difference between surviving species number and Shannon index is even more distinct than in C_{eq} runs: Species numbers reach 1.05±0.22, 1.00±0.00, 2.35±1.31, and 7.35±3.38, in the chemostat and the 3 semi–continuous dilution modes, respectively, indicating a large effect of disturbance on diversity. Yet the Shannon index shows considerably less difference between the different disturbance modes (0.03±0.15, 0.00±0.00, 0.07±0.14 and 0.45±0.45) and considerably lower diversity than in the C_{eq} runs.

In the simulations of virus infections, the results in the C_{eq} runs hardly differ from those in the simple chemostat simulations. We conclude that the virality and frequency of simulated virus attacks was too low to have a reducing effect on diversity by eliminating the infected species, i.e. an infected species simply declined and then recovered without any effect on the final state of the system other than intermittently releasing some nutrients. In the C_{Redf} runs, the frequent infections (every year) even had an unexpected positive effect on diversity: while the chemostat simulations result in a single dominant species, in the virus mortality simulations the dominant species is infected and therefore decimated frequently enough for one inferior competitor to prevail. Hence the mild density–dependence imposed on the random choice of the species to be infected resulted in a slightly higher diversity compared to the chemostat (2.20 ± 0.95 species vs. 1.05 ± 0.22).

4.4.2 Biomass and resource levels

In chemostat or semi–continuous batch culture experiments without the presence of grazers, phytoplankton biomass can be used as an indicator of phytoplankton primary production. Biomass, here calculated in carbon units, is generally expected to be higher

in more diverse communities (Tilman et al., 2001; Striebel et al., 2009). In the present setup, this feature is directly linked to resource use efficiency, i.e. the amount of carbon biomass produced per unit nutrient supplied (see also Ptacnik et al., 2008): Since nutrient supply and dilution rates are identical between different diversity levels and between C_{Redf} and C_{eq} configurations, as are initial total biomass and nutrient concentrations, any differences in biomass between diversity levels or between C_{Redf} and C_{eq} configurations are attributable to differences in resource use efficiency.

The amount of biomass produced per unit resource used depends on phytoplankton stoichiometry, i.e. how much of the limiting resource is needed to assimilate a given amount of C. In the C_{Redf} simulations, the amount of biomass produced per unit resource is always the same, regardless of the (initial) diversity, since stoichiometry is always identical both within and between the different model runs. Differences in productivity arise solely from the dynamics of the model, e.g. between different disturbance modes. In contrast, the C_{eq} runs exhibit a positive relation between diversity and productivity (see figure 4.4 a). The different levels of diversity shown are generated through differences in initial species number, while keeping total initial biomass constant across treatments. Thus, the increase in produced biomass with increasing species number is due to the so–called complementarity effect, i.e. a mixture of species with different resource supply niches allows for more effective resource utilisation than a monoculture (also called overyielding, see e.g. Fridley, 2001).

This effect shows even more clearly in the resource levels (see figure 4.4 b): the more species present, the lower the average normalised resource concentration. Both measures of system productivity reach saturation around the maximum equilibrium diversity of four species, which is to be expected. Any further increase in productivity or resource use efficiency at higher levels of diversity is attributed to the sampling effect, i.e. the increasing chance of sampling species with a particularly high biomass–to–resource ratio. This chance is obviously higher in more diverse assemblies as they can only be attained with higher initial species numbers.

In the C_{Redf} runs, resource concentration is directly linked to carbon biomass, i.e. any resource not taken up by phytoplankton is left in the system. Hence, low resource levels indicate effective resource uptake. Figure 4.5 shows annually averaged concentrations of left–over resources, normalised by their respective inflow concentration for

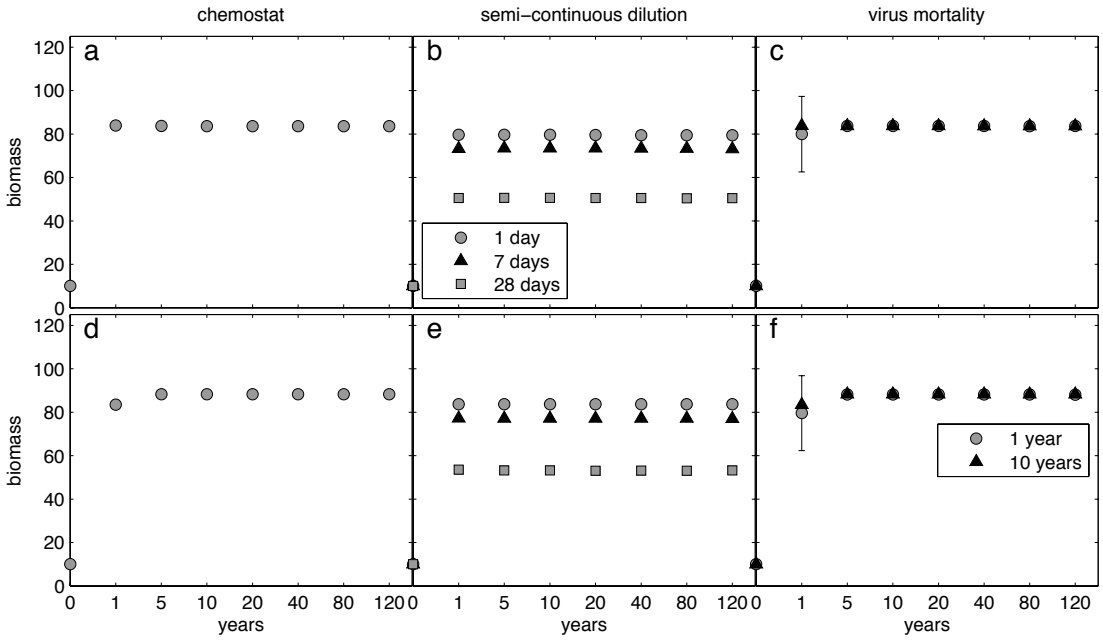

Figure 4.3: 40 species on 4 resources; annually averaged biomass after 1, 5, 10, 20, 40, 80 and 120 years, respectively, mean and standard deviation of replicate runs. Top row: simulations using equilibrium conditions on stoichiometry (C_{eq}), bottom row: Redfield stoichiometry (C_{Redf}). The different disturbance modes are: (a),(d) perfect chemostat; (b),(e) semi–continuous culture with dilution every 1, 7, 28 days; (c),(f) chemostat with "virus infection" every 1 and 10 years.

clarity. Annually averaged left–over resource concentrations are generally much higher in semi–continuous culture simulations than in any other setup: Immediately after a dilution event, resource levels are extremely high, especially for longer dilution intervals, and phytoplankton only gradually reduces the levels.

4.5 Discussion

The different ways to increase phytoplankton diversity in the model experiments reported above can be categorised into stabilising and equalising mechanisms according to Chesson (2000): Stabilising mechanisms enable long–term coexistence of different

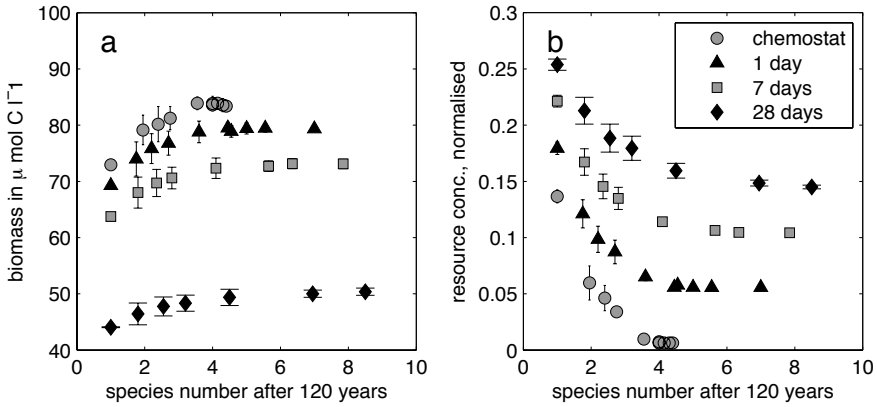

Figure 4.4: 1, 2, 3, 4, 8, 16, 24, 40, 80 and 120 species on 4 resources: averaged remaining diversity vs. system productivity, i.e. mean and standard deviation of (a) total biomass and (b) normalised resource concentration after 120 years (annual average), in C_{eq} simulations in the chemostat and in semi–continuous culture with dilution every 1, 7 and 28 days. Symbols represent disturbance modes, 10 diversity levels per disturbance mode. Missing points are due to truncated x–axes.

species, whereas equalising mechanisms alone can only delay competitive exclusion. A stabilising mechanism leads to intraspecific competition being greater than interspecific competition, an equalising mechanism reduces fitness differences between species.

Disturbance can enable long–term coexistence if species differ in their respective response to disturbance, i.e. if weak competitors under steady–state conditions are strong competitors under disturbance and vice versa, thus providing a disturbance–dependent stabilising mechanism. Since our model does not contain differential responses to disturbance, the superior competitor is superior with and without disturbance and will eventually dominate. In this context, it becomes obvious that dilution events as intermittent disturbance can temporarily promote diversity through reducing the competition between those species that are limited by the same resource, but competitive exclusion will eventually lead to extinction of the inferior competitor(s): Differences between species' growth rates owing to different R*s lead to corresponding differences in biomass. The effect of the dilution events is to minimise those differences, the extent of which increases with increasing dilution intensity and hence, dilution interval. For example in the 28–day

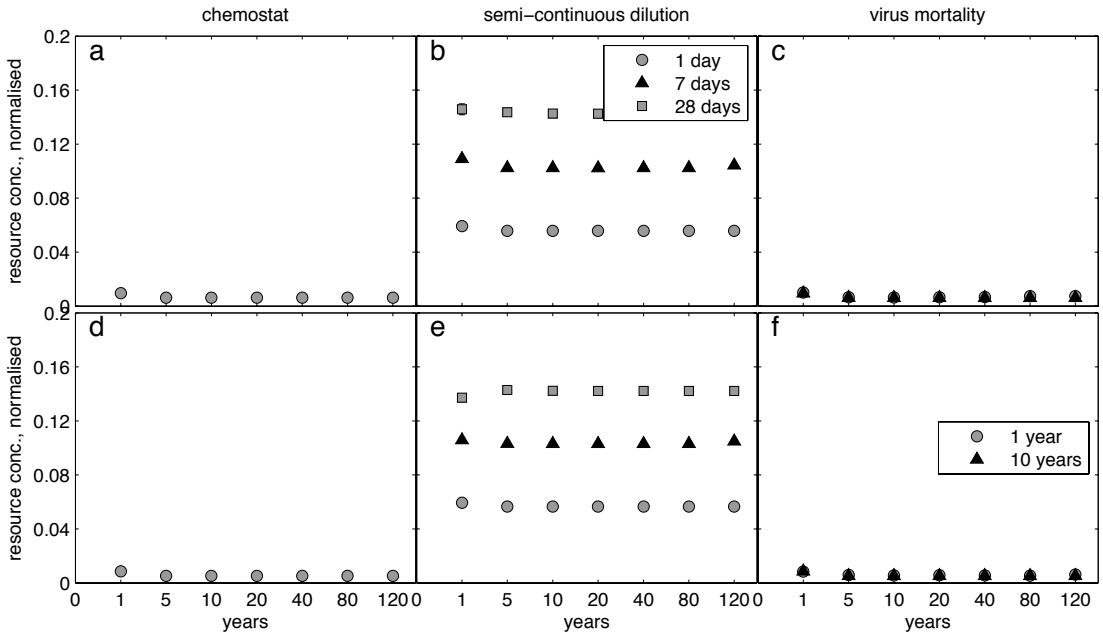

Figure 4.5: 40 species on 4 resources; annually averaged resource concentration after 1, 5, 10, 20, 40, 80 and 120 years, respectively, mean and standard deviation of replicate runs. Top row: simulations using equilibrium conditions on stoichiometry (C_{eq}), bottom row: Redfield stoichiometry (C_{Redf}). The different disturbance modes are: (a),(d) perfect chemostat and chemostat with density–dependent mortality; (b),(e) semi–continuous culture with dilution every 1, 7, 28 days; (c),(f) chemostat with "virus infection" every 1 and 10 years.

interval setup, dilution events remove 99.91% of the biomass, leaving only a miniscule absolute difference in biomass between stronger and weaker competitors. Based on the different growth rates and hence increasing absolute differences in pre–dilution biomass with time, the post–dilution difference also increases with time, eventually leading to competitive exclusion. For shorter intervals, dilution intensity is lower, hence the minimising effect of the biomass removal is weaker, leaving larger differences between strong and weak competitors. Thus, competitive exclusion occurs faster with shorter dilution intervals.

In the C_{eq} runs, species parameters already incorporate a stabilising mechanism: by consuming most of the resource by which it is limited, a species limits itself and its own growth rate more than it limits others, hence intraspecific competition is greater than interspecific competition. Consequently, species stably coexist via differential nutrient utilisation, which is a bottom-up effect. Stabilisation of coexistence can also occur via top-down effects, such as the weakly density–dependent mortality imposed in the virus mortality setup. Coexistence is facilitated in the virus mortality configuration with infections every year for the C_{Redf} runs: the dominant competitor of (usually) two remaining species is decimated frequently enough to allow for the inferior competitor to prevail. Recovery of the inferior species is aided by the re–release of nutrients from the infected species, which is an equalising mechanism *sensu* Chesson (2000). In the C_{eq} runs, the bottom–up mediated diversity through stoichiometric variation dominates the weak top–down effect: the communities consist of mostly four species coexisting at comparable levels of biomass. Since there is no single dominant species, the virus attacks occur rather randomly and cannot prevent competitive exclusion of inferior competitors.

The finding that under semi-continuous dilution events simulated diversity increases with increasing disturbance, albeit only temporarily, is in line with experimental results by Grover (1988), but stands in contrast with the intermediate disturbance hypothesis (IDH, Grime, 1973; Connell, 1978). It is also in contrast with the findings of Barton et al. (2010) according to which diversity was highest in least disturbed regions of the ocean. The IDH does not apply in our setting, because it requires the classical gleaner-opportunist trade-off to be implemented in the species' parameters, whereas our model's phytoplankton consists entirely of gleaners, i.e. species with low half-saturation constants. Additionally, Barton found high diversity in regions of strong lateral advection, i.e. where water masses and hence phytoplankton communities from different ocean regimes mix. This implies that immigration is a strong driver of diversity in the global model used by Barton et al. (2010) and Göthlich and Oschlies (2012). Under semi-continuous dilution, competitive exclusion in our model can take tens of years: with 40 initial species and a one-week disturbance interval, which is thought to mimic e.g. weather events, 14.4 ± 2.3 species are still present after 40 years. Hence, if immigration, which is here simulated through a high number of initial species, is added to the equalising effect of intermittent disturbance, high diversity can persist in the ocean.

We conclude that the increase of diversity with disturbance in our model is due to the disturbance acting as an equalising mechanism *sensu* Chesson (2000), enabling coexistence of several species per limiting resource during timescales close to those in the real ocean, whereas over very long timescales, the long–term equilibrium dominates the system.

4.6 Conclusion

The postulate that interspecific stoichiometric variation increases phytoplankton diversity is held and even fortified through applying external disturbance. In addition to the diversity added via the equalising effect of disturbances, the higher diversity via the stabilising effect of the C_{eq} stoichiometry is maintained, thereby further increasing phytoplankton diversity (see also table 4.5 for summarised results). The positive effects of diversity such as higher resource use efficiency through niche complementarity can only be attained under stable coexistence, which further emphasises the potential benefits of using species-specific stoichiometry in plankton models. Modelling stoichiometry according to a common stoichiometric ratio such as the Redfield ratio does not only impede diversity, but also causes the loss of an important ecological mechanism: even if diversity can be modelled through neutral coexistence, the diversity-productivity relation is still lost. The same holds true for resource use efficiency, which is increased for increased diversity under parameterisation according to equilibrium conditions.

measure	chemostat	semi 1	semi 7	semi 28	virus 1	virus 10
sp no C_{eq}	4.30±0.57	5.00±0.65	7.85±1.53	10.95±1.43	5.40±1.67	4.35±0.67
sp no C_{Redf}	1.05±0.22	1.00±0.00	2.35±1.31	7.35±3.38	2.20±0.95	1.50±0.69
Shannon C_{eq}	1.32±0.10	1.35±0.10	1.43±0.13	1.54±0.17	1.44±0.18	1.33±0.08
Shannon C_{Redf}	0.03±0.16	0.00±0.00	0.07±0.14	0.45±0.45	0.50±0.31	0.13±0.26
biomass C_{eq}	83.56±1.17	79.41±0.98	73.10±0.84	50.49±0.50	83.67±0.82	83.69±0.91
biomass C_{Redf}	88.28±0.004	83.65±0.00	76.98±0.00	53.19±0.01	88.08±0.005	88.28±0.11
resource C_{eq}	0.006±0.00	0.056±0.00	0.104±0.00	0.143±0.001	0.008±0.001	0.006±0.00
resource C_{Redf}	0.005±0.002	0.057±0.001	0.105±0.001	0.142±0.001	0.006±0.002	0.005±0.002
sat C_{eq}	1.11±0.17	1.52±0.29	2.41±0.31	2.86±0.35	1.45±0.30	1.13±0.17
sat C_{Redf}	0.33±0.12	0.25±0.00	0.85±0.39	1.95±0.88	0.59±0.22	0.39±0.17

Table 4.5: Results of 40-species runs after 120 years, mean and standard deviation

4.7 Appendix: Calculation of dilution intensity

Dilution intensity was calculated so that the average growth rate needed to balance the losses (critical growth rate, μ_{crit}) caused by dilution was constant, as proposed by Sommer (1995). Thus, the change of dilution intensity with respect to the dilution interval ($\frac{d\,(V_{\text{ex}}/V_0)}{d\tau}$) equals the relative growth rate of phytoplankton ($\frac{d\,P}{P\,d\tau}$, note that nutrient limitation and additional mortality is not considered):

$$\frac{d\,(V_{\text{ex}}/V_0)}{d\tau} = \frac{d\,P}{P\,d\tau} \tag{4.4}$$

which in turn is dependent on the fraction of medium remaining in the culture vessel $(1 - V_{\text{ex}}/V_0)$:

$$\frac{d\,P}{P\,d\tau} = \mu_{\text{crit}}(1 - V_{\text{ex}}/V_0) \tag{4.5}$$

This yields

$$\frac{d\,(V_{\text{ex}}/V_0)}{d\tau} = \mu_{\text{crit}}(1 - V_{\text{ex}}/V_0) \tag{4.6}$$

Long term dilution, to be consistent with the chemostat parameters, is constant at 25%/day:

$$\frac{d\,V_{\text{ex}}/V_0}{d\tau} = 0.25\,(1 - V_{\text{ex}}/V_0) \tag{4.7}$$

hence V_{ex}/V_0 is determined by integrating equation 4.7 with respect to τ:

$$\int \frac{1}{1 - V_{\text{ex}}/V_0}\frac{d\,(V_{\text{ex}}/V_0)}{d\tau}d\tau = \int 0.25\,d\tau \tag{4.8}$$

$$\Leftrightarrow -\frac{1}{\tau}\ln\,(1 - V_{\text{ex}}/V_0) = 0.25 \tag{4.9}$$

$$\Leftrightarrow V_{\text{ex}}/V_0 = 1 - \mathrm{e}^{-0.25\,\tau} \tag{4.10}$$

5 Conclusions and outlook

Marine biogeochemical models are an important tool in assessing the ocean's response to climate change. During the last few years, these models have undergone considerable refinement with regard to the representation of the pelagic ecosystem. While the first pelagic ecosystem models contained a single state variable for each of the model compartments such as phytoplankton or zooplankton, recent developments include representations of phytoplankton diversity. A fundamental assumption of classical pelagic ecosystem models is that phytoplankton elemental composition is fixed at the Redfield Ratio. This assumption implicitly includes another critical assumption, namely that growth and nutrient uptake are tightly coupled, which in reality they are not.

In this thesis, the impacts of these two assumptions on models employing different ways of representing phytoplankton diversity have been investigated. Two ways of resolving for phytoplankton diversity can be distinguished: (1) explicitly modelling different phytoplankton types or functional groups, i.e. using community–resolving models; (2) modelling the phytoplankton community as a single adaptive phytoplankton whose physiological characteristics adapt to environmental conditions in a way that mimics succession.

In chapter 2 of this dissertation, the effects of coupling vs. uncoupling phytoplankton growth and nutrient uptake, or phytoplankton N and C, were investigated in an adaptive ecosystem model (Pahlow et al., 2008). It was shown that the predictive power of an adaptive model with dynamically adjusting N:C can be considerably impeded if phytoplankton N:C is instead fixed and the model otherwise left as is.

The model investigated in chapter 3 explicitly resolves many phytoplankton species (Follows et al., 2007), all with identical fixed stoichiometric ratios. Despite the high initial diversity, frequently a single species outcompetes all or most of its competitors in one region, with sustained species numbers being lower than the number of limiting re-

sources. It was shown that allowing for different phytoplankton species to have different stoichiometric ratios allows for a higher level of sustained diversity. The exact parameterisation is based on Tilman's resource competition theory and results in differential resource use, hence creating different ecological niches for different species.

Since the theory used to sustain diversity in chapter 3 is based on assuming steady–state conditions, in chapter 4, the relevance of the approach under disturbance was investigated in a chemostat model. It was shown that Tilman's resource competition theory is indeed valid for disturbed systems. Additionally, it was shown that within the framework of resource competition theory, disturbance can enhance species coexistence, albeit not indefinitely, with longer disturbance intervals causing longer periods of high diversity. This result stands in contrast with the intermediate disturbance hypothesis, which states that diversity should be highest at intermediate levels of disturbance (Grime, 1973), and which has been confirmed for plankton in the laboratory (Sommer, 1995) and in lakes (Flöder and Sommer, 1999). On the other hand, patterns of diversity in the model used in chapter 3 show highest diversity in least disturbed areas such as the oligotrophic gyres (Barton et al., 2010), with the exception of diversity "hot spots" where species from different areas are mixed. The sustained diversity under near steady–state conditions is explained by competitive equivalence of the surviving species, hence competitive exclusion does not occur during the timescales under consideration. This explanation has in turn been challenged on the basis of the intermediate disturbance hypothesis (Huisman, 2010). Interestingly, both Huisman and Barton used essentially the same simple chemostat model to make their respective points that is used in chapter 4, but employed a slightly different disturbance mode.

This discrepancy in explanations for disturbance–diversity relationships shows that the underlying mechanisms for the distribution of plankton types and communities are not yet fully understood. Future work on this field of research should include a systematic comparative analysis of disturbance modes, intensities and intervals on phytoplankton coexistence in a simple model.

Generally, the advantage of simple models is that they are straightforward to analyse and the causes for specific results can usually be found. On the other hand, simplification can always lead to key processes being left out such that the results do not reflect observations. This dichotomy between necessary simplification, which is in fact

the point of building a model of any sort, not only mathematical, and oversimplification, which involves the exclusion of key mechanisms and characteristics, is at the heart of any model development. One prime example is the widespread and continuous use of Monod kinetics for nutrient uptake and the Redfield Ratio for stoichiometric coefficients: both concepts are easy to grasp and are valid to some degree, the Monod kinetics for steady–state conditions, the Redfield Ratio in an average over conditions and species. Another advantage is that they require neither a lot of computational power nor many parameter values. Yet the dysfunctionality for especially the combination of these two assumptions with regard to non–steady–state conditions has been shown repeatedly (Flynn, 2010).

One major criticism is that predetermined parameters impede any sort of physiological adaptation of the phytoplankton to variations in its environment, either spatially or temporally. This issue has been addressed in the Follows et al. (2007) model, where a multitude of phytoplankton types is initially present that form communities and biogeographical provinces based to their respective parameter combinations. Yet this model still employs both Redfield and Monod parameterisations, and while model simulations display remarkable agreement with observational data (Follows et al., 2007; Dutkiewicz et al., 2009; Barton et al., 2010), the adaptive potential of a model not allowing for stoichiometric variation is likely limited. Adaptive potential can be improved by increased numbers of coexisting species, which was achieved in this study, but the adaptive potential of models involving adaptive physiology is probably higher. Adaptive models, such as the optimality–based model of Pahlow et al. (2008), resolve for physiological detail, but at the cost of a higher number of state variables and parameters per phytoplankton. Community–resolving models, on the other hand, have only one state variable per phytoplankton, but a much higher number of total phytoplankton state variables. Simplification in the sense of reducing real–world complexity to a computer program can take many approaches and the key question always remains: which processes to include to make the model realistic, and which ones to leave out to keep it a simple as possible –but not simpler, to paraphrase a famous saying attributed to Einstein.

Both the models investigated in this thesis exhibit remarkable qualities with regard to reproducing observations. The Pahlow et al. (2008) has already been extended to include phosphorus Pahlow and Oschlies (2009). Further assessment of model power would include coupling it to a 3–D circulation model and comparing its ability to reproduce global observational data with that of the Follows et al. (2007) model. The latter, on

the other hand, could be extended to include intraspecifically varying stoichiometry, e.g. with the Droop (1973) growth model, as a response to environmental conditions. Especially the distribution of species, communities and diversity in the thus extended model would make a great subject of further research.

Bibliography

Aksnes, D., and J. Egge. 1991. A theoretical model for nutrient uptake in phytoplankton. Marine Ecology Progress Series **70**:65–72.

Anderson, T. 2005. Plankton Functional Type Modelling: Running Before We Can Walk? Journal of Plankton Research **27**:1073–1081.

Anderson, T., and P. Pondaven. 2003. Non-redfield carbon and nitrogen cycling in the Sargasso Sea: pelagic imbalances and export flux. Deep-Sea Research Part I **50**:573–591.

Arhonditsis, G., and M. Brett. 2004. Evaluation of the current state of mechanistic aquatic biogeochemical modeling. Marine Ecology Progress Series **271**:13–26.

Armstrong, R. 2006. Optimality-based modeling of nitrogen allocation and photoacclimation in photosynthesis. Deep-Sea Research Part II: Topical Studies in Oceanography **53**:513–531.

Armstrong, R., and R. McGehee. 1980. Competitive exclusion. American Naturalist **115**:151–170.

Barton, A., S. Dutkiewicz, G. Flierl, J. Bragg, and M. Follows. 2010. Patterns of Diversity in Marine Phytoplankton. Science **327**:1509–1511.

Behl, S., A. Donval, et al. 2011. The relative importance of species diversity and functional group diversity on carbon uptake in phytoplankton communities. Limnology and Oceanography **56**:683–694.

Behrenfeld, M., R. O'Malley, D. Siegel, C. McClain, J. Sarmiento, G. Feldman, A. Milligan, P. Falkowski, R. Letelier, and E. Boss. 2006. Climate-driven trends in contemporary ocean productivity. Nature **444**:752–755.

Boyce, D., M. Lewis, and B. Worm. 2010. Global phytoplankton decline over the past century. Nature **466**:591–596.

Bruggeman, J., and S. Kooijman. 2007. A biodiversity-inspired approach to aquatic ecosystem modeling. Limnology and Oceanography **52**:1533–1544.

Cardinale, B., K. Matulich, D. Hooper, J. Byrnes, E. Duffy, L. Gamfeldt, P. Balvanera, M. O'Connor, and A. Gonzalez. 2011. The functional role of producer diversity in ecosystems. American Journal of Botany **98**:572–592.

Caswell, H. 1978. Predator-mediated coexistence: a nonequilibrium model. American Naturalist **112**:127–154.

Chase, J., P. Abrams, J. Grover, S. Diehl, P. Chesson, R. Holt, S. Richards, R. Nisbet, and T. Case. 2002. The interaction between predation and competition: a review and synthesis. Ecology Letters **5**:302–315.

Chesson, P. 2000. Mechanisms of Maintenance of Species Diversity. Annual Review of Ecology and Systematics **31**:343–366.

Chesson, P., and J. Kuang. 2008. The interaction between predation and competition. Nature **456**:235–238.

Connell, J. 1978. Diversity in Tropical Rain Forests and Coral Reefs. Science **199**:1302–1310.

Denman, K. 2003. Modelling planktonic ecosystems: parameterizing complexity. Progress in Oceanography **57**:429–452.

Doney, S., D. Glover, and R. Najjar. 1996. A new coupled, one-dimensional biological-physical model for the upper ocean: Applications to the JGOFS Bermuda Atlantic Time-series Study (BATS) site. Deep-Sea Research Part II **43**:591–624.

Droop, M. 1973. Some thoughts on nutrient limitation in algae. Journal of Phycology **9**:264–272.

Dutkiewicz, S., M. Follows, and J. Bragg. 2009. Modeling the Coupling of Ocean Ecology and Biogeochemistry. Global Biogeochemical Cycles **23**:GB4017.

Ebenhöh, W. 1994. Competition and coexistence: modelling approaches. Ecological modelling **75**:83–98.

Edwards, A., and A. Yool. 2000. The role of higher predation in plankton population models. Journal of Plankton Research **22**:1085–1112.

Eppley, R. 1972. Temperature and phytoplankton growth in the sea. Fishery Bulletin **70**:1063–1085.

Evans, G., and J. Parslow. 1985. A model of annual plankton cycles. Biological Oceanography **3**:327–347.

Falkowski, P., R. Barber, and V. Smetacek. 1998. Biogeochemical controls and feedbacks on ocean primary production. Science **281**:200–206.

Falkowski, P., R. Scholes, E. Boyle, J. Canadell, D. Canfield, J. Elser, N. Gruber, K. Hibbard, P. Högberg, S. Linder, et al. 2000. The global carbon cycle: a test of our knowledge of earth as a system. Science **290**:291–296.

Fasham, M. 1995. Variations in the seasonal cycle of biological production in subarctic oceans: A model sensitivity analysis. Deep-Sea Research Part I **42**:1111–1149.

Fasham, M., H. Ducklow, and S. McKelvie. 1990. A nitrogen-based model of plankton dynamics in the oceanic mixed layer. Journal of Marine Research **48**:591–639.

Fasham, M., J. Sarmiento, R. Slater, H. Ducklow, and R. Williams. 1993. Ecosystem behavior at Bermuda Station"S"and Ocean Weather Station"India": A general circulation model and observational analysis. Global Biogeochemical Cycles **7**:379–416.

Fleming, R. 1939. The control of diatom populations by grazing. Journal du Conseil **14**:210–227.

Flöder, S., and U. Sommer. 1999. Diversity in planktonic communities: An experimental test of the intermediate disturbance hypothesis. Limnol. Oceanogr **44**:1114–1119.

Flynn, K. 2001. A mechanistic model for describing dynamic multi-nutrient, light, temperature interactions in phytoplankton. Journal of Plankton Research **23**:977–997.

Flynn, K. 2003. Modelling multi-nutrient interactions in phytoplankton; balancing simplicity and realism. Progress in Oceanography **56**:249–279.

Flynn, K. 2010. Ecological modelling in a sea of variable stoichiometry: Dysfunctionality and the legacy of Redfield and Monod. Progress in Oceanography **84**:52–65.

Follows, M., and S. Dutkiewicz. 2011. Modeling diverse communities of marine microbes. Annual Review of Marine Science **3**:427–451.

Follows, M., S. Dutkiewicz, S. Grant, and S. Chisholm. 2007. Emergent biogeography of microbial communities in a model ocean. Science **315**:1843–1846.

Fridley, J. 2001. The influence of species diversity on ecosystem productivity: how, where, and why? Oikos **93**:514–526.

Frost, B. 1987. Grazing control of phytoplankton stock in the open subarctic Pacific Ocean: A model assessing the role of mesozooplankton, particularly the large calanoid copepods *Neocalanus spp.* Marine Ecology Progress Series **39**:49–68.

Gaedeke, A., and U. Sommer. 1986. The influence of the frequency of periodic disturbances on the maintenance of phytoplankton diversity. Oecologia **71**:25–28.

Geider, R., and J. La Roche. 2002. Redfield revisited: variability in the N:P ratio of phytoplankton and its biochemical basis. European Journal of Phycology **37**:1–17.

Geider, R., H. MacIntyre, and T. Kana. 1998. A dynamic regulatory model of phytoplanktonic acclimation to light, nutrients, and temperature. Limnology and Oceanography **43**:679–694.

Gentleman, W. 2002. A chronology of plankton dynamics in silico: how computer models have been used to study marine ecosystems. Hydrobiologia **480**:69–85.

Gentleman, W., and A. Neuheimer. 2008. Functional responses and ecosystem dynamics: how clearance rates explain the influence of satiation, food-limitation and acclimation. Journal of Plankton Research **30**:1215.

Goldman, J., J. McCarthy, and D. Peavey. 1979. Growth rate influence on the chemical composition of phytoplankton in oceanic waters. Nature **279**:210–215.

Göthlich, L., and A. Oschlies. 2012. Phytoplankton niche generation by interspecific stoichiometric variation. Global Biogeochemical Cycles **26**:GB2010.

Gregg, W., N. Casey, and C. McClain. 2005. Recent trends in global ocean chlorophyll. Geophysical Research Letters **32**:L03606.

Gregg, W., P. Ginoux, P. Schopf, and N. Casey. 2003. Phytoplankton and iron: validation of a global three-dimensional ocean biogeochemical model. Deep-Sea Research Part II: Topical Studies in Oceanography **50**:3143 – 3169.

Grime, J. 1973. Competitive exclusion in herbaceous vegetation. Nature **242**:344–347.

Grover, J. 1988. Dynamics of competition in a variable environment: experiments with two diatom species. Ecology **69**:408–417.

Hardin, G. 1960. The competitive exclusion principle. Science **131**:1292–1297.

Hays, G., A. Richardson, and C. Robinson. 2005. Climate change and marine plankton. Trends in Ecology & Evolution **20**:337–344.

Henson, S., R. Sanders, and E. Madsen. 2012. Global patterns in efficiency of particulate organic carbon export and transfer to the deep ocean. Global Biogeochemical Cycles **26**:GB1028.

Hoegh-Guldberg, O., and J. Bruno. 2010. The Impact of Climate Change on the World's Marine Ecosystems. Science **328**:1523.

Holling, C. 1973. Resilience and stability of ecological systems. Annual review of ecology and systematics **4**:1–23.

Hooper, D., F. Chapin III, J. Ewel, A. Hector, P. Inchausti, S. Lavorel, J. Lawton, D. Lodge, M. Loreau, S. Naeem, et al. 2005. Effects of biodiversity on ecosystem functioning: A consensus of current knowledge. Ecological Monographs **75**:3–35.

Howard, M., A. Winguth, C. Klaas, and E. Maier-Reimer. 2006. Sensitivity of ocean carbon tracer distributions to particulate organic flux parameterizations. Global Biogeochemical Cycles **20**:GB3011.

Huisman, J. 2010. Comment on "Patterns of diversity in marine phytoplankton". Science **329**:512–512.

Huisman, J., and F. Weissing. 1999. Biodiversity of plankton by species oscillations and chaos. Nature **402**:407–410.

Huisman, J., and F. Weissing. 2001. Biological conditions for oscillations and chaos generated by multispecies competition. Ecology **82**:2682–2695.

Hutchinson, G. 1961. The paradox of the plankton. The American Naturalist **95**:137.

Keller, D., A. Oschlies, and M. Eby. 2012. A new marine ecosystem model for the University of Victoria Earth System Climate Model. Geoscientific Model Development **5**:1195–1220.

Klausmeier, C., E. Litchman, T. Daufresne, and S. Levin. 2004. Optimal nitrogen-to-phosphorus stoichiometry of phytoplankton. Nature **429**:171–174.

Kriest, I., S. Khatiwala, and A. Oschlies. 2010. Towards an assessment of simple global marine biogeochemical models of different complexity. Progress in Oceanography **86**:337–360.

Laws, E., P. Falkowski, W. Smith Jr, H. Ducklow, and J. McCarthy. 2000. Temperature Effects on Export Production in the Open Ocean. Global Biogeochemical Cycles **14**:1231–1246.

Le Quéré, C., S. Harrison, C. Prentice, E. Buitenhuis, O. Aumont, L. Bopp, H. Claustre, C. Da Cunha, R. Geider, X. Giraud, et al. 2005. Ecosystem dynamics based on plankton functional types for global ocean biogeochemistry models. Global Change Biology **11**:2016–2040.

Leibold, M. 1995. The niche concept revisited: mechanistic models and community context. Ecology **76**:1371–1382.

Litchman, E., and C. Klausmeier. 2008. Trait-based community ecology of phytoplankton. Annual Review of Ecology, Evolution, and Systematics **39**:615–639.

Litchman, E., C. Klausmeier, O. Schofield, and P. Falkowski. 2007. The role of functional traits and trade-offs in structuring phytoplankton communities: scaling from cellular to ecosystem level. Ecology Letters **10**:1170–1181.

MacArthur, R. 1955. Fluctuations of animal populations and a measure of community stability. Ecology **36**:533–536.

McCann, K. 2000. The diversity–stability debate. Nature **405**:228–233.

Michaels, A., A. Knap, R. Dow, K. Gundersen, R. Johnson, J. Sorensen, A. Close, G. Knauer, S. Lohrenz, and V. Asper. 1994. Seasonal patterns of ocean biogeochemistry at the US JGOFS Bermuda Atlantic time-series study site. Deep-Sea Research Part I, Oceanographic Research Papers **41**:1013–1038.

Moloney, C., M. Bergh, J. Field, and R. Newell. 1986. The effect of sedimentation and microbial nitrogen regeneration in a plankton community: a simulation investigation. Journal of Plankton Research **8**:427–445.

Monod, J. 1949. The growth of bacterial cultures. Annual Reviews in Microbiology **3**:371–394.

Monteiro, F., S. Dutkiewicz, and M. Follows. 2011. Biogeographical controls on the marine nitrogen fixers. Global Biogeochemical Cycles **25**:GB2003.

Monteiro, F., M. Follows, and S. Dutkiewicz. 2010. Distribution of diverse nitrogen fixers in the global ocean. Global Biogeochemical Cycles **24**:GB3017.

Naeem, S., and S. Li. 1997. Biodiversity enhances ecosystem reliability. Nature **390**:507–509.

Narwani, A., J. Berthin, and A. Mazumder. 2009. Relative importance of endogenous and exogenous mechanisms in maintaining phytoplankton species diversity. Ecoscience **16**:429–440.

Oschlies, A., and V. Garçon. 1999. An eddy-permitting coupled physical-biological model of the North Atlantic 1. Sensitivity to advection numerics and mixed layer physics. Global Biogeochemical Cycles **13**:135–160.

Pahlow, M. 2005. Linking chlorophyll-nutrient dynamics to the Redfield N: C ratio with a model of optimal phytoplankton growth. Marine Ecology Progress Series **287**:33–43.

Pahlow, M., and A. Oschlies. 2009. Chain model of phytoplankton P, N and light colimitation. Marine Ecology Progress Series **376**.

Pahlow, M., A. Vézina, B. Casault, H. Maass, L. Malloch, D. Wright, and Y. Lu. 2008. Adaptive model of plankton dynamics for the North Atlantic. Progress in Oceanography **76**:151–191.

Palmer, J., and I. Totterdell. 2001. Production and export in a global ocean ecosystem model. Deep-Sea Research Part I, Oceanographic Research Papers **48**:1169–1198.

Peters, F. 1994. Prediction of planktonic protistan grazing rates. Limnology and Oceanography **39**:195–206.

Petersen, R. 1975. The paradox of the plankton: An equilibrium hypothesis. The American Naturalist **109**:35–49.

Polovina, J., E. Howell, and M. Abecassis. 2008. Ocean's least productive waters are expanding. Geophysical Research Letters **35**:L03618.

Popova, E., A. Coward, G. Nurser, B. de Cuevas, M. Fasham, and T. Anderson. 2006. Mechanisms controlling primary and new production in a global ecosystem model–Part I: Validation of the biological simulation. Ocean Science **2**:249–266.

Prowe, A., M. Pahlow, S. Dutkiewicz, M. Follows, and A. Oschlies. 2012. Top-down control of marine phytoplankton diversity in a global ecosystem model. Progress in Oceanography **101**:1–13.

Ptacnik, R., A. Solimini, T. Andersen, T. Tamminen, P. Brettum, L. Lepistö, E. Willén, and S. Rekolainen. 2008. Diversity predicts stability and resource use efficiency in natural phytoplankton communities. Proceedings of the National Academy of Sciences **105**:5134–5138.

Raven, J., and P. Falkowski. 1999. Oceanic sinks for atmospheric CO_2. Plant, Cell & Environment **22**:741–755.

Redfield, A. 1934. On the proportions of organic derivatives in sea water and their relation to the composition of plankton; in: James Johnston memorial volume. University Press of Liverpool.

Richardson, A., and D. Schoeman. 2004. Climate impact on plankton ecosystems in the Northeast Atlantic. Science **305**:1609–1612.

Riebesell, U., A. Körtzinger, and A. Oschlies. 2009. Sensitivities of marine carbon fluxes to ocean change. Proceedings of the National Academy of Sciences **106**:20602–20609.

Riley, G. 1946. Factors controlling phytoplankton populations on Georges Bank. Journal of Marine Research **6**:54–73.

Riley, G., 1984. Reminiscences of an Oceanographer. Unpublished manuscript.

Riley, G., and D. Bumpus. 1946. Phytoplankton-zooplankton relationships on Georges Bank. Journal of Marine Research **6**:33–47.

Riley, G., H. Stommel, and D. Bumpus. 1949. Quantitative ecology of the plankton of the western North Atlantic. Bulletin of the Bingham Oceanographic Collection **12**:1–169.

Roy, S., and J. Chattopadhyay. 2007. Towards a resolution of 'the paradox of the plankton': A brief overview of the proposed mechanisms. Ecological complexity **4**:26–33.

Sabine, C., R. Feely, N. Gruber, R. Key, K. Lee, J. Bullister, R. Wanninkhof, C. Wong, D. Wallace, B. Tilbrook, et al. 2004. The oceanic sink for anthropogenic CO_2. Science **305**:367–371.

Sarmiento, J., T. Hughes, R. Stouffer, and S. Manabe. 1998. Simulated response of the ocean carbon cycle to anthropogenic climate warming. Nature **393**:245–249.

Sarmiento, J., R. Slater, R. Barber, L. Bopp, S. Doney, A. Hirst, J. Kleypas, R. Matear, U. Mikolajewicz, P. Monfray, et al. 2004. Response of ocean ecosystems to climate warming. Global Biogeochemical Cycles **18**:GB3003.

Sarmiento, J., R. Slater, M. Fasham, H. Ducklow, J. Toggweiler, and G. Evans. 1993. A seasonal three-dimensional ecosystem model of nitrogen cycling in the North Atlantic euphotic zone. Global Biogeochemical Cycles **7**:417–450.

Schartau, M., and A. Oschlies. 2003. Simultaneous data-based optimization of a 1D-ecosystem model at three locations in the North Atlantic: Part I—Method and parameter estimates. Journal of Marine Research **61**:765–793.

Scheffer, M., S. Rinaldi, J. Huisman, and F. Weissing. 2003. Why plankton communities have no equilibrium: solutions to the paradox. Hydrobiologia **491**:9–18.

Schmittner, A., A. Oschlies, X. Giraud, M. Eby, and H. Simmons. 2005. A global model of the marine ecosystem for long-term simulations: Sensitivity to ocean mixing, buoyancy forcing, particle sinking, and dissolved organic matter cycling. Global Biogeochemical Cycles **19**:GB3004.

Schneider, B., L. Bopp, M. Gehlen, J. Segschneider, T. Frolicher, P. Cadule, P. Friedlingstein, S. Doney, M. Behrenfeld, and F. Joos. 2008. Climate-induced interannual variability of marine primary and export production in three global coupled climate carbon cycle models. Biogeosciences **5**:597–614.

Shoresh, N., M. Hegreness, and R. Kishony. 2008. Evolution exacerbates the paradox of the plankton. Proceedings of the National Academy of Sciences **105**:12365–12369.

Sinha, B., E. Buitenhuis, C. Quéré, and T. Anderson. 2010. Comparison of the emergent behavior of a complex ecosystem model in two ocean general circulation models. Progress in Oceanography **84**:204–224.

Smith, S., and Y. Yamanaka. 2007. Optimization-based model of multinutrient uptake kinetics. Limnology and Oceanography **52**:1545–1558.

Sommer, U. 1991. A comparison of the Droop and the Monod models of nutrient limited growth applied to natural populations of phytoplankton. Functional Ecology **5**:535–544.

Sommer, U. 1995. An experimental test of the intermediate disturbance hypothesis using cultures of marine phytoplankton. Limnology and Oceanography **40**:1271–1277.

Steele, J. 1958. Plant production in the northern North Sea. Marine Research **7**.

Steele, J. 1974. The structure of marine ecosystems. Harvard University Press Cambridge, Massachusetts.

Steele, J. 1976. The role of predation in ecosystem models. Marine Biology **35**:9–11.

Steele, J., and B. Frost. 1977. The structure of plankton communities. Philosophical Transactions of the Royal Society of London, B, Biological Sciences **280**:485–534.

Steinberg, D., C. Carlson, N. Bates, R. Johnson, A. Michaels, and A. Knap. 2001. Overview of the US JGOFS Bermuda Atlantic Time-series Study (BATS): a decade-scale look at ocean biology and biogeochemistry. Deep-Sea Research Part II, Topical Studies in Oceanography **48**:1405–1447.

Striebel, M., S. Behl, and H. Stibor. 2009. The coupling of biodiversity and productivity in phytoplankton communities: consequences for biomass stoichiometry. Ecology **90**:2025–2031.

Sunda, W., and D. Hardison. 2010. Evolutionary tradeoffs among nutrient acquisition, cell size, and grazing defense in marine phytoplankton promote ecosystem stability. Marine Ecology Progress Series **401**:63–76.

Sunda, W., and S. Huntsman. 1995. Iron uptake and growth limitation in oceanic and coastal phytoplankton. Marine Chemistry **50**:189–206.

Tilman, D. 1980. Resources: a graphical-mechanistic approach to competition and predation. The American Naturalist **116**:362.

Tilman, D., and J. Downing. 1994. Biodiversity and stability in grasslands. Nature **367**:363–365.

Tilman, D., P. Reich, J. Knops, D. Wedin, T. Mielke, and C. Lehman. 2001. Diversity and productivity in a long-term grassland experiment. Science **294**:843–845.

Volterra, V. 1926. Fluctuations in the abundance of a species considered mathematically. Nature **118**:558–560.

von Liebig, J. 1840. Die organische Chemie in ihrer Anwendung auf Agricultur und Physiologie. Friedrich Vieweg und Sohn, Braunschweig.

Wroblewski, J. 1980. A simulation of the distribution of *Acartia clausi* during Oregon Upwelling, August 1973. Journal of Plankton Research **2**:43–68.

Yodzis, P. 1981. The stability of real ecosystems. Nature **289**:674–676.

Yool, A., E. Popova, and T. Anderson. 2011. Medusa-1.0: a new intermediate complexity plankton ecosystem model for the global domain. Geoscientific Model Development **4**:381–417.

Acknowledgements

Thank you...

...Andreas, for being a Doktorvater; for help, guidance, patience, encouragement, challenges, discussions and ideas; for getting me into modelling in the first place; and for the fact that nothing organisational I came up with ever turned into a problem, including working from wherever I happened to be at the time.
...Markus, for providing model codes and countless Matlab routines, for help, discussions, and for frequently coming up with a different point of view.
...Fi, for modelling support and for discussions about science in general and modelling in particular.
...Nora, for being both a colleague and a friend.
...The entire BM team –you're a wonderful group to work in, I'm glad to be part of it.
...Rike, for talks, hugs and being there.
...Meike, Hedi, Kirsten, Micha, for inventing the best way of spending a weekend two days before handing in.
...Stephanie and Ursula for proofreading.
...The folks from the Tea Room, for peace and quiet. And tea.
...My parents, for continuous support.
...Little Nora, for changing everything; and for learning to accept that Mama frequently had to go "aabeiten" on the "pyoota", which would then go "beep" way too often.
...Stephan for Everything.

Hiermit erkläre ich, dass die Abhandlung - abgesehen von der Beratung durch die meinen Betreuer - nach Inhalt und Form meine eigene Arbeit ist. Die Arbeit hat weder ganz noch in Teilen anderer Stelle bereits im Rahmen eines Prüfungsverfahrens vorgelegen. Die Arbeit ist unter Einhaltung der Regeln guter wissenschaftlicher Praxis der Deutschen Forschungsgemeinschaft entstanden.